M-Pos538

AN AMPHIPATHIC α-HELICAL PEPTIDE DIMER DESIGNED FOR MEMBRANE FUSION. ((A. Sen, R. Balakrishnan, H. Iijima, A.L. Kazim, R. Parthasarathy and S.W. Hui)) Roswell Park Cancer Institute, Buffalo, NY 14263.

Amphipathic peptides which destabilize lipid bilayers can cause fusion between opposing biological membranes. It occurred to us that a higher efficiency of fusion may be realized by a disulfide linked dimer with suitable relative orientation of the helical axes in the two halves, so as to insert into and destabilize adjacent membranes. Based on analysis of known viral fusion peptides, Brasseur and co-workers(Biochim. Biophys. Acta 1029:267(1990)) have proposed that for an amphipathic α-helical peptide to be capable of inducing membrane fusion, the peptide has to have a gradient in its hydrophobic moment both along and around the helix axis. Such gradients in the hydrophobic moment of an α-helical peptide will cause the peptide to insert obliquely into and disrupting the lipid bilayer. We have designed a 14 residue peptide, Ac-GGDRAAibEGAibAKAibLL-NH_2, to form an amphipathic α-helix. The peptide was synthesized on an ABI model 431A peptide synthesizer using suitably protected fmoc amino acids. Following synthesis, the peptide was purified using preparative reversed phase HPLC and examined using amino acid analysis, peptide sequencing and FAB mass spectrometry. We first examined the helix propensity of the 14-mer. CD measurements of the peptide showed that there was 24% and 51% α-helix in aqueous buffer (5mM HEPES, pH7) and in trifluroethanol respectively. The peptide was also found to bind to and destabilize erythrocyte membranes. Since the 14-mer formed a helix and destabilized the membrane, we added a Cys residue at the N-terminus of the peptide. By air-oxidation we have prepared a disulfide linked dimer of this peptide. The structure and fusion activities of the monomer and of the dimer are currently under investigation.

A TALE OF TWO MOTORS: MYOSIN AND KINESIN

Tu-AM-SymI-1

THE STRUCTURE OF THE NUCLEOTIDE BINDING SITE IN MYOSIN SUBFRAGMENT-1. ((I. Rayment)) Univ. of Wisconsin.

Tu-AM-SymI-2

MUTATIONAL ANALYSIS OF MYOSIN. ((H.L Sweeney)) Univ. of Pennsylvania Sch. of Med.

Tu-AM-SymI-3

X-RAY DIFFRACTION STUDIES ON NCD AND KINESIN MOTOR DOMAINS. ((R. FLETTERICK)) Univ. of California, San Francisco.

Tu-AM-SymI-4

THE BEST OF TIMES AND THE WORST OF TIMES: FROM MEASUREMENT TO MECHANISM IN KINESIN MOTORS. ((S. BLOCK.)) Princeton Univ.

Tu-AM-A1

BLOCKING EXPRESSION OF THE IP3 RECEPTOR IN HUMAN T CELLS PREVENTS INTRACELLULAR CALCIUM RELEASE
((E. Ondriasova, T. Jayaraman, K. Ondrias, D. Harnick, and A.R. Marks)) Molecular Medicine Program, Mount Sinai School of Medicine, NY, NY 10029

The inositol 1,4,5-trisphosphate receptor (IP3R) is a member of the intracellular Ca release channel superfamily. IP3Rs are widely expressed, however their cellular role is not well understood in many tissues. We have cloned the 10 kb cDNA encoding the human type 1 IP3R from T lymphocytes. To investigate the role of the IP3R in T cells (Jurkat) we blocked its expression using antisense cDNA to generate stable transfectants that do not express IP3R. The IP3R antisense transfected T cells (T-IP3R) had normal levels of T cell receptor (TCR) but did not release intracellular Ca in response to CD3 antibody. The T-IP3R cells could be activated by PMA plus ionomycin, indicating that the signaling pathway for T cell activation was otherwise intact. Depletion of intracellular Ca stores with thapsigargin stimulated Ca influx in the absence of the IP3R, indicating that Ca influx across the plasma membrane does not occur via the IP3R. Cell growth and ^{3}H thymidine incorporation were reduced by ~70% in the T-IP3R cells, indicating that the IP3R may play a role in cell growth but is not required. These results show that the IP3R is critical for T cell activation via the TCR and that Ca influx across the plasmamembrane, triggered by intracellular Ca release, does not involve the IP3R.

Tu-AM-A2

DIRECT INVOLVEMENT OF INTRACELLULAR Ca2+-TRANSPORT ATPase IN THE DEVELOPMENT OF THAPSIGARGIN RESISTANCE BY CHL FIBROBLASTS. **((A. Hussain, C. Garnett, M. G. Klein, J. Tsai-Wu, M. F. Schneider and G. Inesi)) Department of Biological Chemistry, and Oncology Division of the Department of Medicine, University of Maryland School of Medicine, Baltimore, MD 21201.**

Thapsigargin (TG), a specific inhibitor of intracellular Ca2+ transport ATPases (SERCA), inhibits cell proliferation when added to culture media in the nanomolar concentration. Long-term exposure to gradually increasing concentrations of TG induces resistance to TG in both the parental Chinese hamster lung (CHL) fibroblast DC-3F, and a sub-line derived from it via transfection and stable expression of a full-length cDNA encoding avian SERCA1 ATPase. TG resistance is accompanied by high levels of expression of the endogenous SERCA2 as well as the exogenous transfected SERCA1 ATPase. Microsomes isolated from resistant cells contain two populations of ATPases: one sensitive and one resistant to TG. Overexpression of sensitive and resistant ATPase isoforms is an adaptive response to selective pressure, and plays a prominent role in sustaining signaling mechanisms that allow proliferation of resistant cells in TG. (NIH and VA support).

Tu-AM-A3

BLOCKING EXPRESSION OF THE IP3 RECEPTOR IN HUMAN T CELLS PREVENTS INTRACELLULAR CALCIUM RELEASE
((E. Ondriasova, T. Jayaraman, K. Ondrias, D. Harnick, and A.R. Marks)) Molecular Medicine Program, Mount Sinai School of Medicine, NY, NY 10029

The inositol 1,4,5-trisphosphate receptor (IP3R) is a member of the intracellular Ca release channel superfamily. IP3Rs are widely expressed, however their cellular role is not well understood in many tissues. We have cloned the 10 kb cDNA encoding the human type 1 IP3R from T lymphocytes. To investigate the role of the IP3R in T cells (Jurkat) we blocked its expression using antisense cDNA to generate stable transfectants that do not express IP3R. The IP3R antisense transfected T cells (T-IP3R) had normal levels of T cell receptor (TCR) but did not release intracellular Ca in response to CD3 antibody. The T-IP3R cells could be activated by PMA plus ionomycin, indicating that the signaling pathway for T cell activation was otherwise intact. Depletion of intracellular Ca stores with thapsigargin stimulated Ca influx in the absence of the IP3R, indicating that Ca influx across the plasma membrane does not occur via the IP3R. Cell growth and ^{3}H thymidine incorporation were reduced by ~70% in the T-IP3R cells, indicating that the IP3R may play a role in cell growth but is not required. These results show that the IP3R is critical for T cell activation via the TCR and that Ca influx across the plasmamembrane, triggered by intracellular Ca release, does not involve the IP3R.

Tu-AM-A4

MAITOTOXIN ACTIVATES A NON-SELECTIVE CATION CHANNEL IN MOUSE FIBROBLASTS. ((I. D. Dukes, M.S. McIntyre, and J.F. Worley III)) Glaxo Research Institute, RTP, NC 27709.

Maitotoxin (MTX), a marine toxin isolated from the dinoflagellate *Gambierdiscus toxicus*, has been shown to increase intracellular Ca^{2+} ($[Ca^{2+}]_i$) in a variety of cell types. More recently, this toxin has been shown to activate non-selective cation channels in mouse pancreatic β-cells and in a renal epithelial cell line (MDCK). Here we report that maitotoxin activates a non-selective cation channel and increases $[Ca^{2+}]_i$ in a mouse fibroblast cell line (LMTK$^-$). In fura-2 AM loaded fibroblasts, maitotoxin (250-500pg/ml) increased $[Ca^{2+}]_i$ from basal levels around 100nM to above 500nM. This increase in $[Ca^{2+}]_i$ was dependent on Ca^{2+} influx as removal of extracellular Ca^{2+} lowered $[Ca^{2+}]_i$ back to basal levels. Using the perforated patch technique, the effects of MTX on whole-cell membrane currents was examined. In these experiments, the patch pipette contained 120μg/ml nystatin, 70 $CsSO_4$, 30CsCl, 7 $MgCl_2$, 10 HEPES, and the external solution was 145 NaCl, 5KCl, 1 $MgCl_2$, 2 $CaCl_2$, 10 HEPES and 10 glucose Under these conditions, MTX activated a current that reversed at potentials between -20 and 0mV, indicating that the toxin induced a non-selective cation current. This was reversibly inhibited by 5mM Ni^{2+} and by >1 μM of the receptor mediated Ca^{2+} entry blocker SK & F 96365. Using on-cell patches to measure single channel events, MTX (1ng/ml) in the patch pipette activated a nominally quiescent channel that also demonstrated non-selective permeation properties. Addition of SK & F 96365 also blocked MTX induced elevations in fibroblast $[Ca^{2+}]_i$. We conclude that MTX elevates $[Ca^{2+}]_i$ in fibroblasts via activation of a non-selective cation channel freely permeable to Ca^{2+}.

Tu-AM-A5

HETEROGENEITY OF INTERCELLULAR COMMUNICATION IN TUMORIGENIC CELL LINES. ((^{1}G.R. Ehring, ^{2}C. Sun, ^{2}R. Antoniono, and ^{2}J.L. Redpath)) ^{1}Dept of Physiology and Biophysics, ^{2}Dept. of Radiation Oncology, UC Irvine, CA 92717.

We examined tumorigenicity and gap junction-mediated intercellular communication (GJIC) in cell lines cloned from the non-tumorigenic human hybrid *HeLa x Fibroblast* cell line (CGL1) after UV-irradiation. GJIC was measured *in vitro* using the fluorescent recovery after photobleaching (FRAP) assay and tumorigenisis was measured by injecting the cells into nude mice and monitoring the number tumors/injection sites and the rate of tumor growth. Following UV-irradiation, we found that greatly reduced GJIC accompanied rapid tumor growth (UV-12). Some colonies derived from UV-12 expressed increased GJIC and slower tumor growth rates (RM1 & RM101). To test if selection for reduced GJIC and tumorigenisis occurred within the animals, we reconstituted some slowly growing tumors into cell lines and measured their

Cell line	tumors/site	Time to 500 mm^3 tumor (days)	FRAP (GJIC/cells)
CGL1	0/6	n.d.	16/16
UV-12	6/6	13-34	2/22
UV-12 RM1	10/12	48-132	9/9
UV-12 RM101	4/6	90	5/5
UV-12 RM101-0R	4/4	15	9/9

GJIC and their ability to produce tumors when reinjected into mice. The reconstituted cell lines (RM101-0R) showed high levels of GJIC, but produced rapidly growing tumors. These results suggest that high levels of GJIC are not sufficient to prevent tumor growth. Supported by ACS Grant IRG-0166F and NIH Grant R55-CA39312.

Tu-AM-A6

A NOVEL MECHANISM OF ACTION FOR CHEMOSENSITIZING AGENTS. ((Yuri V. Osipchuk, George R. Ehring, and Michael D. Cahalan)) Dept. Physiology and Biophysics, UC Irvine, CA 92717. (Spon. R. Josephson)

Chemosensitizing agents, such as verapamil (VP), are believed to reverse drug resistance by competing with chemotherapeutics for the drug-efflux pump, P-glycoprotein. We examined the mechanism by which VP inhibits the efflux of R123, a fluorescent substrate for P-glycoprotein, in two pairs of drug-sensitive and -resistant cell lines. Video imaging showed that when cells were exposed to 5 μM R123 in the absence of VP, only the drug-sensitive cells accumulated R123. However, in the presence of 10 μM VP both drug-sensitive and -resistant cells took up the dye. Confocal microscopy confirmed that intracellular R123 was primarily localized in intracellular organelles. Following rapid washout of extracellular VP and R123, intracellular R123 decreased with a τ = 260 s. Addition of 10 μM VP slowed R123 efflux 8-fold (τ = 2000 s); this effect was rapidly reversible on washout of VP. Disruption of mitochondrial pH gradients by CCCP (10 μM) augmented R123 efflux (τ = 18 s) when CCCP was applied 200 s after the washout of VP. Confocal microscopy showed that CCCP treatment dispersed R123 from mitochondria and increased its cytoplasmic concentration. Surprisingly, application of CCCP immediately after VP washout only slightly increased the rate of R123 efflux (τ = 146 s) compared with washout alone. Simultaneous addition of 5 mM ATP, but not ATPγS with CCCP restored the effect of CCCP on R123 efflux (τ = 19 s). In addition, confocal microscopy showed that 5 mM ATP prevented intracellular R123 accumulation in the presence of 5 μM R123 and 10 μM VP. Taken together, these results are consistent with the hypothesis that VP stimulates ATP hydrolysis in MDR cells, depleting cytosolic ATP, and in turn impairing pump function. Supported by NIH grant NS14609.

Tu-AM-A7

TWO DIFFERENT CALCIUM-INFLUX PATHWAYS IN MELANOMA CELLS ARE CELL CYCLE-DEPENDENT

((Albrecht Lepple-Wienhues and Michael D. Cahalan)) Department of Physiology and Biophysics, UC Irvine, CA 92717. (Spon. by Stephen H. White)

Melanoma is an aggressive cancer originating from skin melanocytes. We have previously shown that K^+-channel blockers and elevated external $[K^+]_e$ inhibit growth in a human melanoma cell line (SK28). Here, $[Ca^{2+}]_i$ was measured by fura-2 imaging in both G_0-arrested and G_1 cells. Cell cycle stage was studied using PCNA immunostaining and the DNA-probe H33342. We observed two types of Ca^{2+}-influx pathways:

1) Thapsigargin (10^{-6} M) evoked a Ca^{2+}-release activated Ca^{2+} influx (I_{crac}) which was completely blocked by La^{3+}, Gd^{3+} (10^{-6} M) and high $[K^+]_e$ (160 mM). Hyperpolarization by whole-cell patch clamp induced and depolarization inhibited Ca^{2+}-influx in fura-loaded cells. I_{crac} could also be activated by intracellular alkalinization using CO_2-removal or acetate prepulse. I_{crac} was present throughout the cell cycle, but was 2-3 fold greater in G_1 than in G_0.

2) 10% fetal calf serum generated an oscillating Ca^{2+}-rise lasting for 3-4 h while cells entered G_1. In contrast to G_0 cells, high $[K^+]_e$ increased $[Ca^{2+}]_i$ in serum stimulated G_1 cells, implying the induction of voltage-activated Ca^{2+}-channels. This increase was insensitive to nifedipine (10^{-6} M).

We conclude, that at least two different Ca^{2+}-influx pathways are differentially regulated during the cell cycle of melanoma cells.

Supported by NIH grant NS14609 and DFG.

Tu-AM-A8

A THREE-STATE ION-CHANNEL MODEL OF QUANTAL CALCIUM RELEASE BY THE INOSITOL TRISPHOSPHATE RECEPTOR: THEORETICAL PREDICTIONS AND EXPERIMENTAL TESTS.

((R. D. Phair and A. Fayazi)) Department of Biomedical Engineering, The Johns Hopkins University, Baltimore, MD 21205. (Spon. by W.C. Hunter)

Quantal Ca^{2+} release is a novel and incompletely understood gating behavior that is uniquely expressed by intracellular ion channels, particularly the inositol 1,4,5-trisphosphate ($InsP_3$) receptor and the ryanodine receptor. To test proposed mechanisms we built an ion-channel model with one open state and two closed states as shown in the Figure. The model's differential equations were solved for various experimental protocols and were found to reproduce a wide variety of published experimental results, including quantal Ca^{2+} release, transient opening, biphasic Ca^{2+} transport, $InsP_3$-dependence of equilibrium open state probability, apparent desensitization upon $InsP_3$ pretreatment, cold lability of incremental detection, and the bell-shaped dependence of conductance on ambient Ca^{2+}. The model also made the unexpected prediction that two exposures to the *same* concentration of $InsP_3$ separated by a short rest period will result in *two* bursts of Ca^{2+} release. We tested this by measuring $InsP_3$-stimulated ^{45}Ca release from saponin-skinned A7r5 vascular smooth muscle cells. Two bursts of ^{45}Ca were observed experimentally providing additional corroboration of the model and posing a difficult challenge for the original quantal hypothesis.

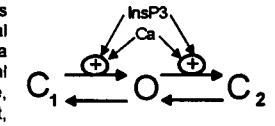

COMPUTER SIMULATIONS/PROTEINS

Tu-AM-B1

PROTEIN SOLVATION: NEW THEORIES AND NEW WATER MODELS.

((T. Ichiye, Y. Liu, J.-K. Hyun and P. D. Swartz)) Department of Biochemistry/Biophysics, Washington State University, Pullman, WA 99164-4660.

Understanding aqueous solvation of proteins is key to understanding their structure and function. A statistical mechanical theory of solvation has previously been described that predicts the structure of water around compact globular molecules such as proteins. This type of theory can thus be used to replace explicit solvation in molecular dynamics and other computer simulations of proteins and in test calculations is about 100 times faster than Monte Carlo simulations. Here, this theory is applied to a new model of water we have developed and comparisons are made to SPC and TIPS-type models of water. This new model of water is about 3 times faster than SPC water in Monte Carlo simulations. Furthermore, an approximate formalism to calculate solvation energies that is similar in spirit to the Born approximation but is valid for arbitrary charge distributions will be presented, with examples for homologous rubredoxins.

Tu-AM-B2

HYDRODYNAMIC PROTEIN INTERACTIONS.

((J.G.E.M. Fraaije, J.T.W.M. Tissen, J. Drenth and H.J.C. Berendsen)) University of Groningen, Nijenborgh 4, 9747 AG Groningen, The Netherlands.

Computer simulations of interacting protein molecules in the early stages of protein crystallization are performed.
Proteins in solution interact via conservative (electrostatic, van der Waals, etc.) and non-conservative (hydrodynamic) forces. Under crystallization conditions, the hydrodynamic interactions (HI) are the only ones acting over a lengthscale comparable with the size of the protein molecules. Furthermore, HI are very important when considering steering effects in the process of nucleation. To study protein crystallization it is therefore of great importance to model these interactions properly.
Using the *Microhydrodynamics* computer simulation technique the hydrodynamic interactions are fully taken into account. For static calculations of the diffusion constants of some proteins, this technique has proven to work well.
Here, we present the method and first results of dynamic simulations of interacting protein molecules, with an emphasis on the effects of the hydrodynamic interactions.

Tu-AM-B3

SIMULATION OF BIOLOGICAL MACROMOLECULES IN AQUEOUS SOLUTION - WITHOUT EXPLICIT WATER MOLECULES

((Gerhard Hummer and Angel E. García)) Theoretical Biology and Biophysics Group T-10, MS K710, Los Alamos National Laboratory, Los Alamos, NM 87545, U.S.A.

We present a new theoretical method that allows to add the solvation energy to existing force-field descriptions of biomolecular interactions without the need of including individual water molecules. The interaction energy with the water environment is expressed as a sum over two-and three-particle interactions involving the strongly polar atoms of the solute molecule. The distance-dependent interaction potentials are extracted from bulk water simulations. As a first test, the alanine dipeptide is studied. Going from vacuum to solution (as modeled with the additional interactions), we observe a shift in the minimum energy structures from the hydrogen bonded C_7 to the more solvent exposed α_R and β structures. The β structure is found to be the most stable, followed by α_R, and then C_7^{ax}, separated by about 1 kcal/mol in each case. These results agree with previous computer simulation studies using explicit water models. Applications of the new method to larger molecules (in particular, folding of peptides and proteins) will be discussed. The use of a modified force field implicitly containing energy contributions owing to the solvent greatly reduces the computational requirements when studying biological macromolecules in solution by computer simulation. This method can be used to analyze the structure and dynamics of large molecules; and it promises to become a powerful tool in studies of biomolecular association (e.g., docking studies) where large molecules are involved and water is known to play an important role.

Tu-AM-B4

EXPLORING THE PROTEIN FOLDING LANDSCAPE: SIMPLE MODEL STUDY OF FOLDING DYNAMICS.

((N.D. Socci and J.N. Onuchic)) Department of Physics, University of California at San Diego, La Jolla CA 92093-0319.

Recent work using simple lattice models have shown that these models capture much of the essence protein folding. The advantage of these models is that they can be studied in great detail so one can determine how the various factors effect folding, both kinetically and thermodynamically. Using a simple three dimensional lattice model we study the free energy surface (landscape) and examine how various properties of this surface, such as roughness, effect the kinetics of folding. The notions of transition states and reaction coordinates are examined, in particular how one can define such concepts on the generally complex reaction landscape of protein folding. Finally, we explore how the sequence of monomers affects the shape and character of the free energy surface and what properties lead to faster folding and more stable structures.

* Supported by the Arnold and Mabel Beckman Foundation, the University of California, San Diego Chancellor's Fellowship (to N.D.S) and the NSF (Grant# MCB9018768).

Tu-AM-B5

LOOKING FOR RAPID-FOLDING STRUCTURES : A LATTICE MODEL STUDY USING OPTIMIZED INTERACTIONS. ((Sridhar Govindarajan and Richard A Goldstein)) Department of Chemistry and Biophysics Research Division, University of Michigan, Ann Arbor, MI 48109.

Nature optimizes protein sequences through evolution to facilitate folding on an adequate time scale. We used lattice models of proteins with optimized interactions. The optimization maximizes the folding temperature of a structure with respect to its glass transition temperature. The folding ability of particular compact structures were studied. Several interesting aspects arose in this study. The structures that have better ability to fold have contacts which are rare in random structures. Optimization of local and nonlocal interactions indicates that a structure is best optimized when the contribution from local interactions to their stability is relatively small. The optimization also induces correlations in the energy landscape of the proteins, stabilizing native like structures with respect to random structures.

Tu-AM-B6

LENS α-CRYSTALLIN QUATERNARY STRUCTURE: A COMPUTER GENERATED MODEL. ((B. Groth-Vasselli[1], T F. Kumosinski[2], and P.N. Farnsworth[1])) UMD-New Jersey Medical School, 185 South Orange Ave., Newark, NJ 07103. [2]Macromolecular and Cell Structure, U.S.D.A, Philadelphia, PA.

The quaternary structure of α-crystallin is the missing link for defining its functions as a structural and chaperone protein on the molecular level. α-Crystallin exists in the lens and other tissues as polydisperse, dynamic heteropolymers with varying ratios of αA and αB subunits (~20KD). In this study, quaternary structures of both hetero and homopolymers of varying molecular weights were constructed by utilizing our computer generated working models of the two subunits and their complex. The elongate, amphipathic nature of these 3-D subunits is best suited for construction of a micellar quaternary structure. The orientation of each subunit is dictated by the assumption that interactions of the hydrophobic N-termini are the driving force for aggregation. The models are "open" spherical micelles which contain an inner cavity defined by the proximal, hydrophobic N-terminal residues. The observed graded increase in aggregate radius with increased molecular weight can be attributed to increases in the diameter of the inner cavity. The hydrophilic C-terminal domain of each subunit is exposed to the surface and imparts aggregate solubility. These quaternary structures are in excellent agreement with the vast literature that has accumulated over the past several decades. Sponsored by UMD-NJ Foundation Grant and RPB, Inc.

Tu-AM-B7

SCATTERING/DIFFRACTION METHODS TO EXTRACT *IN SITU* STRUCTURAL INFORMATION ABOUT PARTICLES IN A MACROMOLECULAR COMPLEX ((Satoru Fujiwara and Robert A. Mendelson)) The Cardiovascular Research Institute and Dept. of Biochemistry and Biophysics, The University of California, San Francisco, CA 94143 (Spon. by R.Fletterick)

Neutron scattering combined with selected isotopic labeling and contrast matching is suitable for obtaining *in situ* structural and distance information about particles in a macromolecular complex. The observed intensities, however, may be distorted by intercomplex interference and by scattering-length-density fluctuations of the (otherwise) density-matched portions. Various methods have been proposed to cancel out such distortions: Hoppe's method (*J. Mol. Biol.* 78: 581-585, 1973), a variation of Hoppe's method (Kneale *et al. Q. Rev. Biophys.* 10: 485-527, 1977) -- here termed the Statistical Labeling Method, and the Triple Isotopic Substitution Method (Pavlov and Serdyuk, *J. Appl. Cryst.* 20: 105-110, 1987). Using these methods, *in situ* structural information can be obtained without these distorting effects. We found that the SLM can be generalized to apply to ordered and oriented systems having any number of labeled particles (Fujiwara & Mendelson, *J. Appl. Cryst.*, in press, 1994). It is also shown that the TISM can be applied to ordered and oriented systems. Thus, all of these methods can be applied to *in situ* structures of systems having underlying symmetry and/or net orientation, as well as to globular particles in solution. The information obtainable from such experiments will be discussed. Other related methods and possible experiments using X-rays will also be discussed. [Supported in part by NIH (R01-AR39710) and NSF (DMB-876091) grants to R.A.M.]

Tu-AM-B8

CONTEXT DEPENDENT OPTIMAL SUBSTITUTION MATRICES DERIVED USING BAYESIAN STATISTICS AND PHYLOGENETIC TREES. ((J.M. Koshi and R.A Goldstein)) Biophysics Research Division and Department of Chemistry, Ann Arbor, MI 48109-1055.

Substitution matrices are a key tool in important applications such as identifying sequence homologies, creating sequence alignments, and more recently using evolutionary patterns for the prediction of protein structure. We have derived a novel approach to the derivation of these matrices that utilizes not only multiple sequence alignments, but also the associated evolutionary trees. The key to our method is the use of a Bayesian formalism, and subsequent ability to approximate the probability that a given substitution matrix fits the tree structures and multiple sequence alignment data. With this ability, we can then evolve optimal substitution matrices for various local environments, depending upon parameters such as secondary structure and surface accessibility. These optimized matrices can then be used as tools to help predict the secondary structure of proteins.

RHODOPSIN—BACTERIORHODOPSIN

Tu-AM-C1

EFFECTS OF THE TRANSDUCER PROTEIN HTRI ON THE EXTRACELLULAR AND CYTOPLASMIC PROTON-CONDUCTING PATHS IN SENSORY RHODOPSIN I. ((J.L. Spudich, E.N. Spudich and B. Perazzona)) Dept. Micro. and Mol. Genet., U. of Tx., Houston, TX 77030

The phototaxis receptor sensory rhodopsin I (SR-I) normally exists in a tight molecular complex with its integral membrane transducer protein HtrI. Spectroscopic data indicates light-induced deprotonation of the Schiff base occurs in the photoactive site of SR-I during HtrI activation, but the proton is not released from the membrane. Removal of HtrI exposes 2 proton-conducting paths: one, the EP, from the Schiff base to the extracellular medium, and a second, the CP, from the cytoplasm to the Schiff base. Both paths exist (at different times) during the HtrI-free SR-I photocycle, and vectorial translocation of the proton from the cytoplasm to the extracellular side occurs. We are conducting deletion analysis of HtrI and site-specific mutagenesis of SR-I to elucidate the mechanism by which HtrI blocks these paths. Two conclusions are that neutralization of Asp76 near the Schiff base by HtrI interaction blocks the EP, and the N-terminal half of HtrI through a yet unknown mechanism is sufficient to block the CP. Extramembranous pH appears to control the reprotonation of the Schiff base through the CP in HtrI-free SR-I, providing a criterion for the presence of this path. In vitro reconstitution with purified SR-I and HtrI is also being developed.

Tu-AM-C2

ELECTROGENIC PROTON-TRANSLOCATION BY ACID AND ALKALINE FORMS OF TRANSDUCER-FREE SENSORY-RHODOPSIN-I. ((W. Stoekenius, I. Szundi, J.G. Fukushima and R.A. Bogomolni)) University of California, Santa Cruz, CA 95064

Transducer-free Sensory Rhodopsin-I, fsR-I, exists in two forms in proton-dependent equilibrium (pK = 7.2). Excitation of the acid form, fsR_{590}, generates a near-UV absorbing sM intermediate with proton release to the intracellular medium. During thermal decay of sM to fsR_{590} proton uptake is rate-limiting and occurs from the same side of the membrane. Excitation of the alkaline species, fsR_{550}, also generates a sM form but with proton release to the outside and uptake from the inside as in bacteriorhodopsin resulting in net outward electrogenic proton pumping. Both the alkaline and acid sM species are reconverted to the ground form by near-UV light with H^+-uptake from the outer surface, which shortcircuits the fsR_{550} pump but results in electrogenic inward H+-pumping for fsR_{590}:

$$fsR_{590} + \text{yellow light} \rightarrow \text{acid-sM} + H^+_{in}$$

$$\text{acid-sM} + \text{near-UV light} + H^+_{out} \rightarrow fsR_{590}$$

We show that simultaneous excitation of fsR-I in cell envelope vesicles (22 °C, 4 M NaCl) with both yellow (500-700nm) and near-UV light (300-400 nm) in the pH range 4.5-6.2 (optimum about 5.2) causes uncoupler-sensitive alkalinization of the medium and generates an inside-positive membrane potential. Above pH 6.5 blue light only reduces the proton extrusion driven by yellow light. At very high light intensities, however, blue light can increase the outward pumping by the fsR_{550} photocycle due to excitation of a photoproduct of its sM intermediate. Supported by NIH GM-43561.

Tu-AM-C3

PHOTOCYCLE OF THE PROTON-PUMPING FORM OF TRANSDUCER-FREE SENSORY-RHODOPSIN-I. ((I. Szundi and R.A. Bogomolni)) Univ. of California Santa Cruz, CA 95064

Sensory Rhodopsin-I free of its transducer Htr1, fsR-I, undergoes a pH-dependent spectral transition: $fsR_{590} \leftrightarrow fsR_{550} + H^+$ (pK = 7.2), which apparently involves Asp76. Both fsR_{550} and fsR_{590} undergo cyclic photoreactions that include spectrally similar intermediates, sM (or S_{373}) with presumably unprotonated Schiff base chromophores (K,L,M,N indicate sR states presumably analogous to the intermediate states of the bacteriorhodopsin, bR, photocycle). The fsR_{550} photoreaction pumps protons out of the cell like bR. Excitation of fsR_{590} does not result in proton translocation, transient protons are both released and taken up on the inner membrane surface. In cell envelope vesicles at ~22 °C the fsR_{550} photoreaction generates two forms ($<10^{-7}$ sec.), sK and sL, which are in fast, kinetically unresolved equilibrium and decay into sM with a half-time of about~$3x10^{-6}$ sec. The sM state reconverts thermally into fsR_{550} with pH dependent kinetics, half-time of ~140 sec. at pH 8.1, in the rate-limiting step of the cycle. The fsR_{590} photocycle is distinct from both the fsR550 and the transducer-complexed csR-I cycle. It includes a K-like intermediate that decays in tens of microseconds to an L-like species. The latter either re-converts to the ground form or gives rise of an M-like intermediate in the 10^{-2} sec. range in a branching reaction similar to that observed for native sR-I at lower temperatures. Supported by NIH GM-4361

Tu-AM-C4

PHOTOINDUCED REORIENTATIONAL MOTION IN THE BACTERIORHODOPSIN PHOTOCYCLE. ((Carey K. Johnson, Greg S. Harms, and Qin Song)) Department of Chemistry, University of Kansas, Lawrence, KS 66045.

Reorientations of bacteriorhodopsin have been detected in the purple membrane by time-resolved linear dichroism measurements. The chromophore is observed to reorient by about 20° during the K→M stages of the bacteriorhodopsin photocycle and to return to the original orientation in the O intermediate. The recovery of an anisotropy of 0.39 in the O state demonstrates that these rotational motions are reversible and not diffusive. Similar reorientational motions of up to 15° are also observed for bacteriorhodopsin immobilized in polyacrylamide gels. A study of the pH dependence of the anisotropies of photocycle intermediates shows that reorientations occur with greatest amplitude at physiological pH, and are virtually eliminated below pH 5 and above pH 9. Photoinduced reorientational motions also occur in neighboring "spectator" (non-photocycling) proteins in the trimer over this pH range. Supported by NIH GM 40071.

Tu-AM-C5

PHOTOLYSIS-INDUCED PK_A INCREASE OF THE CHROMOPHORE COUNTERION IN BACTERIORHODOPSIN: IMPLICATIONS FOR ION TRANSPORT MECHANISMS OF RETINYLIDENE PROTEINS. ((Mark S. Braiman, Kenneth G. Victor, and Jennifer Lewis)) Biochemistry Department, University of Virginia Health Sciences Center, Charlottesville, VA 22908.

In the unphotolyzed state of bacteriorhodopsin (bR), the pK_a of the primary proton acceptor group, Asp-85, is ~2.5, typical of water-exposed carboxylic acids. This is consistent with our determination of a COOH frequency of 1732 cm^{-1}—also typical of water-exposed carboxylic acids—for Asp-85 in FTIR spectra of unphotolyzed $bR_{acid\ purple}$. The Asp-85 COOH vibration shifts to a much higher frequency of 1755-1762 cm^{-1} in the M, N, and/or O photoproducts formed transiently at all pH values from 1 to >10.5. This indicates a photolysis-induced shift in the environment around Asp-85 from very hydrophilic to very hydrophobic. In agreement with this conclusion, we have also observed that Asp-85 is protonated even in the long-lived M- and N-like photoproducts formed at pH =10.5 in the presence of 1 *M* NaCl. Thus, the pK_a of Asp-85 is clearly raised from ~2.5 in unphotolyzed bR to >10.5 in the longest-lived photointermediates. This photolysis-induced change in pK_a is nearly as large as that previously deduced for the chromophore, but in an opposite direction. The crossover in pK_a values of the Schiff base and Asp-85 helps to explain the photolysis-induced proton transfer between them in the M state. The >8-unit pK_a increase, and loss of multiple hydrogen bonds, also correspond to a 40 kJ/mol destabilization of the counteranion relative to the unphotolyzed state. In the related Cl^- pumping protein, halorhodopsin, Asp-85 is replaced by a halide and the Schiff base never deprotonates. Nevertheless, the same photoisomerization-induced destabilization of the counteranion as in bR would generate a transient Cl^--motive force that could help explain light-driven halide transport. *Supported by NIH grant GM46851.*

Tu-AM-C6

A DEUTERIUM-NMR STUDY OF THE RETINAL CHROMOPHORE ORIENTATION IN BACTERIORHODOPSIN DURING THE PHOTOCYCLE. ((Anne S. Ulrich#*, Ingrid Wallat§, Maarten P. Heyn§, and Anthony Watts#)). # Dept of Biochem., University of Oxford, South Parks Road, Oxford OX1 3QU, UK; § Dept of Physics, Freie Universität Berlin, Arnimallee 14, 14195 Berlin, Germany; *Present address: EMBL, Meyerhofstr. 1, 69117 Heidelberg, Germany.

Photo-isomerization of the retinal chromophore leads to proton-translocation through the membrane protein bacteriorhodopsin (BR) in the purple membrane of *H. salinarium*. Since atomic resolution is not yet available for BR or the chromophore, we have developed a solid-state deuterium-NMR technique to determine the tilt angle and molecular conformation of retinal in BR from the orientations of its selectively deuterated methyl-groups [1-3]. The local angle between a labelled C-CD_3 bond and the membrane normal is calculated from the spectral quadrupole splitting of uniaxially oriented purple membrane samples, and by lineshape analysis of a tilt series of spectra. Any movement of the chromophore during the photocycle is described by following the re-orientations of individual molecular segments. Here, we report changes in the chromophore alignment between the initial state and the cryo-trapped key intermediate M_{412}. Upon isomerization from all-*trans* to 13-*cis* retinal, the angle between the central methyl group of the polyene-chain, C_{19}, and the membrane normal increases from 40° (± 1°) in the initial state to ~ 44° (± 2°) in M_{412} [4]. This local change suggests a slight upward tilting of the retinal axis. The bulk of retinal thus remains relatively firmly anchored within the BR binding pocket but may partially compensate for the flip at the Schiff base end.

[1]. Ulrich, A. S., I. Wallat, A. Watts & M.P. Heyn (1994) Biochem. 33, p5370
[2]. Ulrich, A.S. & A. Watts (1993) Solid State Magn. Res. 2, p21
[3]. Ulrich, A. S., M. P. Heyn & A. Watts (1992) Biochem. 31, p10390
[4]. Ulrich, A. S., I. Wallat, M.P. Heyn & Watts, A. (1994) Nature Str. Biol. (submitted)
ASU was funded by MRC (UK) & the EC. SERC (UK) funded the NMR (to AW).

Tu-AM-C7

HYDRATION INDUCED FLEXIBILITY IN BACTERIORHODOPSIN STUDIED BY QUASIELASTIC INCOHERENT NEUTRON SCATTERING (QINS). ((J. Fitter[1,2], G. Büldt[2], N.A. Dencher[3] and R.E. Lechner[1])) [1]Hahn-Meitner Institut, BENSC (NI), Glicnicker Str. 100, D-14109 Berlin; [2]Forschungszentrum Jülich, IBI-2, Biologische Strukturforschung, D-52425 Jülich; [3]Inst. f. Biochemie, TH Darmstadt, Petersenstr. 22, D-64287 Darmstadt

The dynamical behaviour of biological macromolecules on the picosecond timescale is important to understand their functional aspects. These fast stochastic structural fluctuations are essential for slower conformational changes (on a millisecond time scale) occurring in protein structures, which are found to be correlated to the biological function (Koch et al, EMBO J. 10, 521-526, 1991). QINS is a powerful tool to study diffusive motions in a time range from pico- to nano-seconds of hydrogen atoms, which are distributed nearly "uniformly" in biological macromolecules. A QINS study was performed on bacteriorhodopsin using oriented stacks of purple membranes (PM) hydrated at two different levels (0.03 g D2O/g PM; 0.28 g D2O/g PM). With respect to the influence of hydration on the dynamics, we separated diffusive components corresponding to molecular subunits. A three site jump diffusion of protons in methyl groups with a correlation time of about 5 ps was found to be the fastest process. Reorientational diffusive motions of protein side groups were found to be slower (correlation times 15-100 ps) and show a significant spatial anisotropy in the case of low hydration. Contrary to this, no anisotropy was observed for both types of diffusive motions at high hydration and for the three site jump diffusion at low hydration.

Tu-AM-D1

AN ICONOGRAPHY OF AMINO ACIDS BASED ON MUTUAL INFORMATION BETWEEN PROTEIN SEQUENCE AND LOCAL STRUCTURE ((M. J. Thompson and R. A. Goldstein)) Biophysics Research Division and Department of Chemistry, University of Michigan, Ann Arbor, MI 48109-1055

Protein evolution has produced local structural environments that are more conserved than amino acid sequence. Thus, knowledge of the amino acids allowed to occupy a position in a tertiary fold provides insight into the characteristics necessary to maintain that local structure. This information can be obtained from patterns of conservation and variation in alignments of protein homologs. The number of groupings to be considered is reduced from the $2^{21} - 1$ possible patterns of amino acids by considering them as subsets of more general "description classes". Using information theory, the statistical correlations between the patterns in a particular class and the secondary structure environments that they occupy can be quantified as the "mutual information" between the two. A Metropolis search scheme is used to find, for any number of description classes, the configuration with the maximum mutual information. Sets of increasing numbers of classes can then be arranged as "nodes" in hierarchical treelike structures. The information represented in these trees could potentially be useful in protein mutagenesis work and will provide a means of codifying multiple sequence alignment data into a tertiary structure recognition method.

Tu-AM-D2

MULTIFRACTAL ANALYSIS OF SOLVENT ACCESSIBILITIES IN PROTEINS. ((T. Gregory Dewey and James S. Balafas)) Dept. of Chemistry, University of Denver, Denver, CO 80208.

Solvent accessiblities of amino acid side-chains of proteins are analyzed using a multifractal approach. Solvent accessibilities are determined computationally from X-ray crystallographic data. These accessibilities are ordered in sequence according to their corresponding residue along the protein chain. Using a generalized box-counting algorithm, each sequence is shown to exhibit multifractal behavoir. The existence of multifractal spectra indicate correlations between accessibilities and a hierarchical structure to the sequence data.. The multifractal parameters are used to extract an underlying binary multiplicative process with one-step memory. Similar binary processes occur in the generation of helix-coil sequences in biopolymers. Computer simulations were performed that generated misfolded proteins. The misfolded proteins have narrower multifractal spectra than the properly folded ones. Thus, this multifractal analysis can be used as a diagonostic tool in assessing proper folding in structure prediction algorithms.

Tu-AM-D3

TESTS OF A DIELECTRIC MODEL OF SOLVATION FOR THERMAL-LEVEL FREE ENERGY CHANGES UPON CONTINUOUS MOLECULAR REARRANGEMENTS IN WATER. ((Gregory J. Tawa, Lawrence R. Pratt, Gerhard Hummer, Angel E. Garcia)) Theoretical Division, Los Alamo National Laboratory, Los Alamos, NM 87545

We present accurate results of a dielectric model for potentials of the average forces among charged and polar solutes in water for several cases of conformational and reaction equilibrium for which reliable molecular scale information is available. This permits new tests of the dielectric model for predictions of thermal-level free energy changes with continuous molecular scale rearrangements. Examples include (a) conformational equilibrium of the alanine dipeptide, (b) reaction equilibrium for symmetric SN2 attack of methlychloride by chloride ion, (c) reaction equilibrium for SN2 attack of formaldehyde by hydroxide ion, (d) binding of sodium ion to dimethlyphosphate, and (e) pairing of alkali metal and halide ions in water. The molecular statistical thermodynamic theory underlying the dielectric model and directions for further development are commented upon.

Tu-AM-D4

Vibrational analysis of N-methylacetamide (NMA)

R. Schweitzer-Stenner[1], X.G. Chen[2], S.A. Asher[2], N.G. Mirkin[3] and S. Krimm[3]

[1] Institut für Experimentelle Physik, Universität Bremen, D-28334 Bremen,
[2] Department of Chemistry, University of Pitttsburgh, Pittsburgh, PA 15260,
[3] Biophysics Research Division, University of Michigan, Ann Arbor, MI 48109

We have obtained vibrational assignments of aqueous *trans*-NMA and some of its deuterated isotopomers from band decomposition of IR absorption, visible, and resonance Raman spectra. The amide I and II bands of NMA are each composed of two broad bands with different intensities and depolarization ratios. The two amide I subbands (1626 and1646 cm^{-1}) arise from vibrational mixing between the amide I vibration and the bending motions of water molecules hydrogen bonded to the CO - and NH-groups.This coupled motion is likely to have biological significance in areas such as protein structure, energy relaxation and vibrational energy transport. The amide II subbands (at 1566 and 1584 cm^{-1}) are attributed to two, nearly isoenergetic conformers, which differ in the orientation of the N-methyl hydrogens. Moreover we find that even at visible excitation amide III (1314 cm^{-1}) and the band arising from the C-methyl symmetric bending motion (1377 cm^{-1}) exhibit depolarization ratios close to 0.33, which indicates that their intensities are determined by the 190 nm $\pi->\pi^*$ transition. In contrast amide I and II show a dispersion of their depolarization ratios owing to additional contributions to their off-resonance spectra from electronic transitions at shorter wavelengths.

Tu-AM-D5

REFERENCE ATR-FTIR STUDIES OF MEMBRANE-BOUND PEPTIDES AND LINKED ANALYSIS OF POLARIZED SPECTRA

((Paul H. Axelsen & Brad Kaufman))
Department of Pharmacology, University of Pennsylvania, Philadelphia PA

Peptides which assume a known conformation and orientation in oriented lipid membranes were studied in order to test the assumptions commonly made in studies of infrared dichroism. For gramicidin in a supported DMPC monolayer, we determined an order parameter for amide I of 0.3, and this agrees with the value we predict from the crystal structure. In oriented DMPC multilayers, Lys_2-Gly-Leu_{24}-Lys_2-Ala-amide (gift of R. McElhaney), an order parameter in excess of 1.0 is obtained if we assume that it is an α-helix, and that the angle between the transition moment of amide I and the helix axis is ≥34°. Amide I order, and α, are undoubtedly somewhat less than these values, but in any case, the data strongly support an overall helical conformation and orientation perpendicular to the plane of the membrane.

Our analysis of infrared dichroism is aided by a software program which simultaneously bandfits several spectra with the option to link fitting parameters such as band position, width, shape, etc. This was particularly advantageous in the case of gramicidin, in which a band at 1634 cm^{-1} dominated the parallel-polarized spectrum, and another band at 1658 cm^{-1} dominated the perpendicular-polarized spectrum.

Supported by the L. P. Markey Charitable Trust

Tu-AM-D6

INTERACTION OF AMPHIPATHIC HELICAL PEPTIDES WITH MEMBRANES. ((H. W. Huang, K. He, S. J. Ludtke, Y. Wu)) Rice Univ., Houston TX 77251.

A general molecular picture of how amphipathic helical peptides interact with membranes has emerged from experiments of oriented circular dichroism, x-ray diffraction and neutron scattering. The peptides' cytolytic activity is triggered by a phase transition in which the peptides change from a membrane surface state to a membrane insertion state. At low peptide-to-lipid ratio (P/L), the peptides are adsorbed on the hydrophilic-hydrophobic interface, separating the lipid headgroups laterally. By fluctuation, a number of peptides on the surface may aggregate and insert into the bilayer, forming an ion channel. Because of the mismatch between the chain length and the peptide's hydrophobic length, the free energy of the membrane deformation caused by an inserted peptide bundle is high, so the channel has a short lifetime. As the P/L increases, the bilayer thickness decreases in proportion, until P/L reaches a critical value. At this P/L, the peptide starts to insert into the bilayer and the bilayer ceases further thinning--the thickness of the chains becomes equal to the peptide's hydrophobic length. Furthermore the insertion destabilizes the surface peptide, making the insertion a cooperative phenomenon. This general picture can be explained based on the deformation free energy of a bilayer. However, there are important differences between different peptides and between different lipids.

Tu-AM-D7

TRANSLOCATION OF AN ANTIMICROBIAL PEPTIDE, MAGAININ 2, ACROSS LIPID BILAYERS THROUGH FORMING A MULTIMERIC PORE

((K. Matsuzaki, O. Murase, N. Fujii, and K. Miyajima)) *Faculty of Pharmaceutical Sciences, Kyoto University, Sakyo-ku, Kyoto 606-01, Japan*

Magainin 2, an antimicrobial peptide isolated from *Xenopus* skin, kills bacteria by permeabilizing the cell membranes. We have reported [1–3] that magainin preferentially interacts with acidic phospholipids, forming an amphiphilic helix with its axis parallel to the membrane surface and permeabilizing the membrane, although the detailed mechanisms are to be revealed. In this paper, magainin 2 has been shown to translocate across phospholipid bilayers through forming a transient pore comprising of the multimeric peptide. The translocation was proved by four different experiments using resonance energy transfer from tryptophan introduced into the peptide to a dansyl chromophore incorporated into the lipid membrane. The translocation was coupled to the pore formation, as detected by the dye efflux from lipid vesicles. The kinetics of the pore formation also could be well explained by this translocation model.

[1] K. Matsuzaki et al., *Biochim. Biophys. Acta* **981**, 130 (1989).
[2] K. Matsuzaki et al., *Biochim. Biophys. Acta* **1063**, 162 (1991).
[3] K. Matsuzaki et al., *Biochemistry* **33**, 3342 (1994).

Tu-AM-D8

INTERACTIONS BETWEEN BETA-AMYLOID AND ACETYLCHOLINE IN THE DEVELOPMENT OF ALZHEIMER'S DISEASE.

((Gerald Ehrenstein and Zygmunt Galdzicki)) Biophysics Section, NINDS and Laboratory of Neurosciences, NIA, NIH, Bethesda, MD 20892.

We present a model to explain the decrease in acetylcholine (ACh) concentration that is one of the characteristics of Alzheimer's disease. In the model, beta-amyloid acts on membranes of cholinergic neurons to increase the leakage of choline out of the cells [Cf. Galdzicki et al., Brain Research 646 (1994) 332-336]. For a considerable time, this leakage is compensated by increased pumping of choline into the cells. Eventually, a threshold is reached where pumping can no longer keep up with leakage. Then the intracellular choline concentration decreases, resulting in a decrease in ACh production. In the model, the decrease in ACh production also causes an increase in production of beta-amyloid [Cf. Greengard et al., Neurobiology of Aging 15 Supplement 1 (1994) S39]. Thus, there is positive feedback between increases in beta-amyloid production and decreases in ACh production. As a result, after the threshold is reached, ACh production declines relatively rapidly. This model can be approximated by a set of differential equations, and their numerical solution provides estimates of the rapidity of the decline in ACh production.

MECHANISMS OF EXOCYTOSIS

Tu-AM-SymII-1

KINETICALLY RESOLVED SECRETION STUDIES IN ADRENAL CHROMAFFIN CELLS

((E. Neher))
MPI für biophysikal. Chemie, Abt. Membranbiophysik, Göttingen, Germany

Neurosecretory cells, such as chromaffin cells of the adrenal medulla are ideally suited for studying secretory processes, since they are readily accessible experimentally. The whole-cell patch clamp configuration allows to control membrane currents and to load cells with calcium indicator dyes, caged-Ca, and Ca-chelators. Secretion can be studied on the single-cell level by membrane capacitance measurement (assaying changes in surface area during exocytosis) and by electrochemical detection, using carbon microfibers. Experiments at moderate time resolution allowed to characterize a pool of readily releasable vesicles which depletes during stimulation and refills afterwards on a time scale of seconds to minutes. Both the process of refilling and the exocytotic release process are activated by calcium (v. Rüden, Neher, Science 262, 1061-1065, 1993). Applying rapid step increases in $[Ca^{2+}]$, using caged Ca, a quantitative relationship between release-rate and $[Ca^{2+}]$ could be established (Heinemann et al, Biophys. J, 67, 1, 1994), which , in turn, can be used to estimate the effective $[Ca^{2+}]$ at the release site during voltage-pulse depolarizations. It is found that the majority of vesicles 'experience' a peak Ca-concentration of only $\approx 5\mu M$ during 20 msec depolarizations (Chow et al, 1995, PNAS, in press). This is much less than would be expected if Ca-channels and release sites were part of the same macromolecular complex. The values conform with the assumption of mean distances between channels and release sites on the order of 100 nm, as judged by the predictions of model calculations on buffered diffusion of calcium.

Tu-AM-SymII-2

SYNAPTIC VESICLE MEMBRANE FUSION: PROTEINS AND POTENTIAL MECHANISMS. ((T.C. Südhof)) Univ. of Texas Southwestern Med. Ctr.

Tu-AM-SymII-3

LIPID MIXING, PROTEINS, AND KINETICS OF MEMBRANE FUSION. ((J. Zimmerberg)) NIH.

Tu-AM-SymII-4

THE FORMATION AND EVOLUTION OF FUSION PORES.

((F.S. Cohen, G.B. Melikyan, and W.D. Niles)) Department of Molecular Biophysics and Physiology, Rush Medical College, Chicago, IL 60612.

The kinetics of fusion of influenza virus hemagglutinin (HA) expressing cells to planar bilayers and the fusion pores connecting the two membranes are being characterized. After triggering fusion by low pH, there is an electrically quiescent phase followed by formation of fusion pores that repetitively flicker open and closed. Shortly after these pores form, the fluorescent lipid probe rhodamine-PE moves from planar to cell membranes, demonstrating continuity of lipid for flickering pores. A pore then securely opens and eventually enlarges in a step-wise fashion from the nS to μS range, sufficient for release, *in vivo*, of viral nucleocapsids into cytosol. The kinetics of fusion – time from acidification to first pore formation and closed times between flickering pores – quickens with increased density of HA. But once formed, pore properties – open time distributions of flickering and securely open pores and time course of pore enlargement – are independent of HA density. Thus, accretion of HA trimers into the pore is not responsible for pore growth. Analysis of waiting time distributions until fusion indicates that increased HA density speeds both non-rate-limiting and rate-limiting steps leading to fusion. In contrast, mechanical properties, bending moduli and tension, of the membranes that form the walls of the pore affect not only kinetics of pore formation, but also pore growth. Flickering and securely open pores have the same initial conductances and the same early rates of growth, suggesting they evolve from common structures. Supported by NIH GM27367.

Tu-AM-E1

PERIPHERAL COUPLINGS AND TRIADS LACK FEET AND TETRADS IN DYSPEDIC MICE WITH A TARGETED MUTATION OF THE GENE FOR SKELETAL MUSCLE RYANODINE RECEPTOR. ((H. Takekura*, M. Nishi#, T. Noda@, H. Takeshima#, and C. Franzini-Armstrong+)) *NIFS, Kagoshima; # Tokyo Inst. Psychiatry; @Japan Cancer Institute; +U. of Pennsylvania.

A targeted mutation ($skrr^{m1}$) of the gene for skeletal muscle ryanodine receptors (RyRs) results in absence of excitation-contraction (e-c) coupling in homozygous mutants (Takeshima et al., Nature, 369:556, 1994). The mutant gene is expected to produce no functional RyR. In normal muscle, junctions are formed between the sarcoplasmic reticulum (SR) and either the surface membrane or the T tubules. Two structural components of these junctions, the feet of the SR and the tetrads of T tubules have been identified as RyRs, or SR calcium release channels, and as dihydropyridine receptors (DHPRs), or voltage sensors of e-c coupling. We have examined the development of junctions in skeletal muscle fibers from mouse dyspedic embryos, homozygous for the targeted mutation. Surprisingly, despite absence of RyRs, junctions are formed in dyspedic myotubes, but have a narrow junctional gap, presumably because the feet are missing. Tetrads are also absent from these junctions. The results confirm identity of RyRs and feet and a major role for RyRs and tetrads in e-c coupling. The gap in dyspedic junctions is too narrow to accomodate the cytoplasmic domains of RyRs and this excludes the possibility that either the cardiac or the neural isoforms of the protein participate in the formation of these junctions. Since feet and tetrads are missing in dyspedic myotubes and the mutated protein is unlikely to span the junctional gap, coupling of SR to surface membrane and T tubules may be mediated by protein(s) different from either the RyRs the DHPRs.

Tu-AM-E2

RECTIFICATION OF THE CALCIUM RELEASE CHANNEL OF SKELETAL MUSCLE SARCOPLASMIC RETICULUM (RYANODINE RECEPTOR) BY FK506 BINDING PROTEIN 12. ((S. R. Wayne Chen, Lin Zhang and David H. MacLennan)) Banting and Best Department of Medical Research, University of Toronto, Toronto, Canada M5G 1L6

A soluble 12,000 Da FK506 binding protein, FKBP12, the cellular receptor of the immunosuppressive drug, FK506, is tightly associated with the Ca^{2+} release channel of rabbit skeletal muscle sarcoplasmic reticulum (Jayaraman et al. (1992) J. Biol. Chem. 267, 9474-9477). We have assessed the role of excess free FKBP12 in the function of single Ca^{2+} release channels incorporated into planar lipid bilayers. The addition of human recombinant FKBP12 (hFKBP12) to the cytoplasmic face of the Ca^{2+} release channel, blocked the flow of cytoplasmic to luminal current (outward current) in a concentration-dependent manner, but had no significant effect on the flow of luminal to cytoplasmic current (inward current). The luminal to cytoplasmic flow of current was modulated by Ca^{2+}, Mg^{2+}, ATP, caffeine and ryanodine in the presence and absence of hFKBP12. An immunosuppressive drug L-683,590, an analog of FK506, did not block or reverse the hFKBP12 blockade of single Ca^{2+} release channels in planar lipid bilayers. Identification of FKBP12 binding sites on the Ca^{2+} release channel should provide important information concerning structure-function relationships of channel gating. (Supported by the MRC of Canada.)

Tu-AM-E3

LUMINAL Ca^{2+} REGULATES THE OPEN PROBABILITY OF SKELETAL SR Ca^{2+}-RELEASE CHANNELS ACTIVATED BY ATP AND cADP-RIBOSE. ((R. Sitsapesan and A.J. Williams)). NHLI, University of London.

We have demonstrated that activation of the sheep cardiac SR Ca^{2+}-release channel by sulmazole is dependent upon the luminal $[Ca^{2+}]$. In contrast, luminal Ca^{2+} has no effect on the open probability (Po) of channels activated solely by cytosolic Ca^{2+}. We have now investigated if luminal Ca^{2+} can regulate the sheep skeletal SR Ca^{2+}-release channel when activated by cytosolic Ca^{2+}, ATP or cADP-ribose (cADPR). Vesicles of heavy SR were incorporated into planar phospholipid bilayers and current fluctuations through single Ca^{2+}-release channels were recorded in symmetrical 250 mM CsPIPES, pH 7.2; free $[Ca^{2+}]$ 5 μM. The Po of channels activated by cytosolic Ca^{2+} alone (15 μM) was unchanged by increasing the luminal $[Ca^{2+}]$ from picomolar levels to 10 mM at $\pm$40 mV (n=7). However the Po of channels activated by ATP (1 mM) or cADPR (1 & 10 μM) was increased by increasing the luminal $[Ca^{2+}]$. For example, with 1 mM ATP, 1 μM cytosolic Ca^{2+} and 5 μM luminal Ca^{2+}, the Po was 0.199 ± 0.09 at -40 mV and 0.208 ± 0.12 at +40 mV (n=5; SEM). Increasing the luminal $[Ca^{2+}]$ to 2 mM increased Po to 0.874 ± 0.15 at -40 mV and 0.927 ± 0.09 at +40 mV (n=4; SEM). Our results demonstrate that luminal Ca^{2+} regulates the Po of skeletal Ca^{2+}-release channels when activated by certain ligands and may represent a physiological mechanism for inactivation of SR Ca^{2+} current.
This work was supported by the British Heart Foundation.

Tu-AM-E4

FUNCTIONAL PROPERTIES OF THE SKELETAL MUSCLE RYANODINE RECEPTOR EXPRESSED IN *XENOPUS* OOCYTES ((E. Kobrinsky, K. Ondrias, A. Scott, A.-M. Brillantes and A.R. Marks)) Molecular Medicine Program, Mount Sinai School of Medicine, NY, NY 10029

To examine the calcium release channel properties of the skeletal muscle ryanodine receptor (RyR1) and the role of FKBP12 in determining these properties we functionally expressed its cDNA in *Xenopus* oocytes. Two methods were used to study the expressed RyR1 in oocytes. First, we used the Ca-activated chloride current that is native to oocytes as a reporter for intracellular Ca release. Secondly, we removed the intracellular membranes from oocytes expressing RyR1 and fused them to planar lipid bilayers and characterized the single channel properties of RyR1. We compared the properties of the cloned RyR1 to those of the native rabbit skeletal muscle RyR1 protein injected into oocytes. *Xenopus laevis* oocytes do not express FKBP12 mRNA or protein. In the absence of FKBP12 the cloned RyR1 formed a functional intracellular Ca release channel in oocytes that was activated by caffeine, doxorubicin and ryanodine. The cloned RyR1 expressed in oocytes displayed single channel properties that were comparable to those of the native RyR1 including modulation by ryanodine, inhibition by ruthenium red and activation by caffeine and doxorubicin. The cloned channel, in the absence of FKBP12, exhibited multiple subconductance states that were not seen in the native channel or when RyR1 was co-expressed with FKBP12. These studies show that FKBP12 modulates channel gating but is not required for formation of the tetrameric structure or Ca release channel function of RyR1.

Tu-AM-E5

SINGLE CHANNEL PROPERTIES OF THE FULL LENGTH AND TRUNCATED CLONED EXPRESSED RYANODINE RECEPTOR ((K. Ondrias, B.E. Ehrlich*, and A.R. Marks)) Molecular Medicine Program, Mount Sinai School of Medicine, NY, NY 10029 and *Departments of Medicine and Physiology, University of Connecticut, Farmington, CT 06030

To functionally localize regulatory sites on the skeletal muscle ryanodine receptor (RyR) we compared the properties of the full-length cloned expressed RyR with those of a truncated RyR. Recombinant full length and truncated RyR were expressed in insect cells (Sf9), purified and reconstituted into liposomes. To measure the single channel properties, liposomes were fused to planar lipid bilayers. The single channel properties were determined in the presence of 53 mM Ca as the current carrier on the luminal side and 125 mM Tris on the cytoplasmic side of the channel. The conductance of the full length RyR was 103 pS, as measured for the native RyR with Ca as the current carrier, but the channel opened frequently to subconductance levels. These channels were activated by caffeine and ATP, inhibited by ruthenium red, and modified by ryanodine. The truncated RyR was composed of the carboxy half of the molecule which contains all the putative transmembrane regions and a small portion of the foot protein. The conductance of the truncated channel was ~100 pS, but this value was difficult to determine because the channel opened primarily to subconductance levels. The truncated channel was activated by caffeine, inhibited by ruthenium red and modified by ryanodine. These results suggest that the pore forming region of the molecule is fully contained in the carboxy region portion of RyR and that many of the regulatory sites also reside in this region.

Tu-AM-E6

Association of Triadin with the Ryanodine Receptor and Calsequestrin in the Lumen of Sarcoplasmic Reticulum. (Wei Guo and Kevin P. Campbell) Howard Hughes Medical Institute, Department of Physiology and Biophysics, University of Iowa College of Medicine, Iowa City, IA 52242

Triadin is an abundant membrane protein in the junctional sarcoplasmic reticulum of the skeletal muscle. Based upon membrane topology analysis, triadin contains a single transmembrane domain that separates this protein into cytoplasmic and luminal domains. Only the N-terminal 47 amino acids are cytoplasmic with the bulk of triadin including the carboxyl terminus located within the lumen of sarcoplasmic reticulum. The luminal domain contains a high concentration of positively charged amino acids and has been proposed to interact with calsequestrin. In order to identify the proteins in skeletal muscle that interact with triadin, the cytoplasmic domain (C-triadin) and the luminal domain of triadin (L-triadin) were expressed as glutathione-S-transferase (GST) fusion proteins and immobilized to glutathione Sepharose to form affinity columns. The L-triadin Sepharose binds both the ryanodine receptor and calsequestrin from CHAPS-solubilized skeletal muscle homogenates. The luminal but not the cytoplasmic domain of triadin binds [^{3}H] labeled ryanodine receptor, whereas neither the cytoplasmic nor the luminal domains bind [^{3}H]PN-200-100 labeled dihydropyridine receptor. Also, L-triadin interacts with calsequestrin in a Ca^{2+}-dependent manner and is able to inhibit the reassociation of calsequestrin to the junctional face membrane. These results suggest that triadin anchors calsequestrin to the junctional region of sarcoplasmic reticulum, and is involved in the coupling between calsequestrin and the ryanodine receptor/Ca^{2+}-release channel.

Tu-AM-E7

INTERACTIONS OF FKBP12 WITH THE CA^{2+} RELEASE CHANNEL OF RABBIT SKELETAL MUSCLE. ((Kenneth J. Slavik, Dolores Needleman, Jian-Ping Wang, Hemanta Sarkar, Irina Serysheva, *Wah Chiu, #Andrew Marks, and Susan L. Hamilton)). Department of Molecular Physiology and Biophysics, *Department of Biochemistry, Baylor College of Medicine, Houston, TX 77030, #Department of Molecular Biology, Mt. Sinai Medical Center, New York, NY 10029.

A 12kDa protein (FKBP12) which binds the immunosuppressive drug, FK 506, copurifies with the skeletal muscle Ca^{2+} release channel (Jayaraman *et al., J. Biol. Chem.* 267:9474-9477, 1992). FKBP12 can be quantitatively extracted from SR membranes with rapamycin. We have examined the effects of this extraction on 1) ^{3}H-ryanodine binding, 2) tryptic digest patterns, 3) sulfhydryl labeling, and 4) the appearance of the protein by cryoelectron microscopy Our data suggest that the removal of the protein has pronounced effects on the conformation of the Ca^{2+} release channel. We have also expressed the rabbit skeletal muscle FKBP12 in *E. coli* using a pGEX-2T vector. The protein was purified on a glutathione-agarose column, labeled with ^{125}I using iodobeads, and its binding site on FKBP12 depleted SR membranes has been examined.

This work is supported by grants from the Muscular Dystrophy Association and from the National Institutes of Health (AR41802, HL37044, and AR41729). D.N. is a recipient of a National Research Service Award (AR08217).

Tu-AM-E8

3D STRUCTURE OF THE SKELETAL MUSCLE Ca^{2+} RELEASE CHANNEL IN ITS OPEN AND CLOSED STATES BY ELECTRON CRYOMICROSCOPY AND ANGULAR RECONSTITUTION. ((Irina I. Serysheva, Elena V. Orlova*, Michael B. Sherman, Marin van Heel*, Wah Chiu and Susan L. Hamilton)) Department of Biochemistry and Department of Molecular Physiology and Biophysics, Baylor College of Medicine, Houston, TX 77030 ; * Fritz Haber Institute of the Max Plank Society Faradayweg 4-6, D-14195 Berlin, Germany.

The structure of the Ca^{2+}-release channel in two conformational states has been investigated by electron cryomicroscopy. The protein was solubilized with CHAPS and purified from rabbit fast twitch skeletal muscle. By depleting the Ca^{2+} with EGTA, the Ca^{2+}-release channel protein was driven towards its closed state. To determine the 3D structure of the channel protein we exploit the random orientations of the ice-embedded molecules. An exhaustive search of the different characteristic projection images was conducted through an iterative procedure of multi-reference alignment, multivariate statistical analysis and classification procedures and the Euler angle assignment. The resulting 30 Å three-dimensional map of the closed Ca^{2+} release channel reveals a transmembrane region with no opening between the SR lumen and the cytoplasm. The extended cytoplasmic region has a hollow appearance and consists of peripheral mass shaped like a closed clamp at four corners and interconnected by "bridging domains". The "open" state of the channel was obtained in the presence of 100 μM Ca^{2+} and 100 nM ryanodine. The 3D map of the open channel reveals a central hole of 25 Å in diameter in the membrane spanning domain. Pronounced differences were identified in the peripheral mass of the cytoplasmic region as well. The structural transitions in the Ca^{2+}-release channel determined in the presence of Ca^{2+} presumably are associated with the physiological process of channel activation and excitation-contraction coupling.

This work is supported by the W.M.Keck Foundation, the R.Welch Foundation, the Muscular Dystrophy Association of America, the National Institutes of Health and the DFG.

Tu-AM-E9

SELECTIVE INTERACTION OF FKBP-12.6 WITH CARDIAC RYANODINE RECEPTOR ((H. Onoue, A.P. Timerman, H.B. Xin, S. Barg, *G. Wiederrecht and Sidney Fleischer)) Dept. of Mol. Biol., Vanderbilt University, Nashville, TN 37235; *Merck Res. Labs., Rahway, N.J. 07065-0900. (Spon. by J. Venable)

The cardiac calcium release channel (CRC)/ryanodine receptor (RyR-2) from dog heart sarcoplasmic reticulum (SR) is tightly associated with an FK506 binding protein (FKBP-C). FKBP-C is a different isoform (Timerman et al., Biophys Res. Commun., 198, 1994) from human recombinant FKBP-12, which is found associated with skeletal muscle ryanodine receptor (RyR-1). FKBP-C appears to be identical to a novel 12.6-kDa FKBP (FKBP-12.6) characterized from brain by Sewell, et al. (J. Biol. Chem. 269, 1994). In this study, interaction between FKBP-12.6 and cardiac SR was assessed. FKBP-depleted cardiac SR specifically bound recombinant [^{35}S]FKBP-12.6, but not [^{35}S]FKBP-12 (both at 2μM), whereas FKBP depleted skeletal muscle SR bound both. We previously found that FKBP-12 can exchange with [^{35}S] FKBP bound to RyR-1 (Timerman, et., al., Biophys J., in press, 1995). FKBP-12.6 was at least 500 fold more potent than FKBP-12 in exchanging with [^{35}S]FKBP-12.6 bound to the cardiac ryanodine receptor. Thus, we find that FKBP-12.6, but not FKBP-12 preferentially associates with the cardiac ryanodine receptor, even though the cytosol contains mainly FKBP12. (Supported by NIH HL32711 and Muscular Dystrophy Association.)

CHANNEL SELECTIVITY

Tu-AM-F1

ISOLATION OF A SINGLE PROTON-BINDING SITE IN A CYCLIC NUCLEOTIDE-GATED CHANNEL. **((James A. Morrill and Roderick MacKinnon)) Dept. of Neurobiology, Harvard Medical School, Boston, MA 02115.**

Previous work has identified two identical, non-interacting protonation sites in the pore of a cloned cyclic nucleotide-gated channel (CNGC) that govern transitions between proton-dependent subconductance states. These sites, which can be obliterated by mutating the glutamate at position 333 to glycine, titrate with a pKa of 7.6. In one model, a complete channel is formed by four subunits, and the two protonation sites arise from the pairing of the four glutamates into two identical carboxyl-carboxylate moieties. Such a scheme accounts for the equivalence of the sites and the difference between their observed pKa and the pKa of 4-5 that would be expected for carboxyl groups acting alone. One prediction of this model is that it should be possible to alter the protonation sites by inserting glycine-mutant subunits into the channel structure. In particular, it should be possible to disrupt one of the protonation sites while preserving the other intact, a situation that would yield two subconductance states instead of three. The present study tested this prediction by expressing a mixture of wild-type (E333) and mutant (E333G) subunits in Xenopus oocytes, with the goal of creating heteromultimeric channels. Using the inside-out patch clamp technique, single CNGCs were identified and their behavior was compared both to completely mutant channels (no substates) and to completely wild-type channels (three substates). We discovered at least three intermediate types of channels in co-injected oocytes, one of which has two subconductance states, as predicted, with behavior that titrates about pH 7.6. The results suggest that the two protonation sites of this CNGC can be isolated structurally.

Tu-AM-F2

CONDUCTANCE SATURATION IN A CYCLIC-NUCLEOTIDE GATED CHANNEL IS LINKED TO A P-REGION GLUTAMATE RESIDUE. ((Michael J. Root and Roderick MacKinnon)) Program in Biophysics and Department of Neurobiology, Harvard Medical School, Boston, MA, 02115.

Sodium passes through the cyclic-nucleotide gated channel from olfactory epithelium at three distinct current levels. Each level represents a different protonation state of a glutamate cluster (Glu^{333}) in the channel pore. The highest of these conductance states has a linear current-voltage (i-V) relationship and saturates at low ionic strengths. The lower two conductance states have outwardly-rectifying i-V relationships, but still saturate at increasing NaCl concentrations. However, when Glu^{333} is replaced by Gly, this single conductance-state channel shows marked outward rectification but its conductance does not saturate up to sodium concentrations of 1 M. These results suggest that the Glu^{333} cluster, already known to form a divalent cation binding site, also forms a sodium binding site close to the extracellular mouth of the channel.

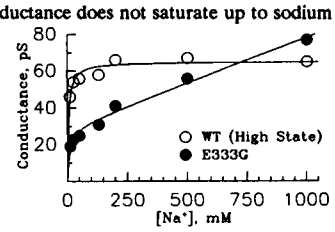

Tu-AM-F3

DIVALENT CATION SELECTIVITY OF AN ION BINDING SITE IN THE PORE OF A CYCLIC NUCLEOTIDE-GATED CHANNEL. **((Chul-Seung Park and Roderick MacKinnon)) Department of Neurobiololgy, Harvard Medical School, Boston, MA 02115.**

The effects of external divalent cations on Na^+ currents through cyclic nucleotide-gated (CNG) channels were studied in patches excised from *Xenopus* oocytes expressing the channel. While divalent cations permeate the channel, they also block current carried by monovalent cations. A Glu residue at position 363 is known to mediate this blockade by extracellular divalent cations. By measuring the blockade of Na^+ currents under conditions where a divalent cation permeates minimally, we studied the selectivity of the binding site formed by Glu 363. A strong size selectivity is observed in that Ca^{2+} is bound more tightly than Mg^{2+} or Sr^{2+}. In addition, when the binding site is modified by replacing Glu 363 with Asp, not only are the absolute affinities for the three metal ions changed, but also the selectivity pattern is altered. These results show that the CNG channel pore is selective among divalent cations in a manner similar to Ca^{2+} channels and some previously described metal binding sites in proteins of known structure.

Tu-AM-F4

TUNING THE DEGREE OF RECTIFICATION BY ADJUSTING THE INTERNAL PROTON CONCENTRATION IN A HISTIDINE MUTANT CHANNEL OF ROMK1. **((Zhe Lu and Roderick MacKinnon)) Department of Neurobiology, Harvard Medical School, MA 02115.**

Inward-rectifier K^+ channels rectify mainly because of voltage-dependent blockade by intracellular cations of which Mg^{2+} is one of the major contributors. Using site-directed mutagenesis, a single residue at position 171 in ROMK1 that affects Mg^{2+} affinity was identified. The residue appears to have its effect through an electrostatic mechanism and therefore must be near the Mg^{2+} binding site. We have now characterized the ROMK1 channel with a histidine at 171 (N171H). The degree of rectification can be tuned even in the absence of Mg^{2+} by adjusting internal pH: rectification occurs as pH is decreased below 9. By contrast, the wild-type channel does not exhibit pH-dependent rectification. The inhibition of mutant channel currents by protons at a given membrane voltage can be described by the equation, $I/I_o = K_i(V)/(K_i(V)+[H^+])$, as if a single proton induces blockade. The blockade is voltage-dependent with a valence of 0.37. We propose that the side-chain of residue 171 faces the ion conduction pore at a site 40% across the transmembrane potential difference.

Tu-AM-F5

FUNCTIONAL ROLE OF A CONSERVED ASPARTATE IN THE EXTERNAL MOUTH OF VOLTAGE-DEPENDENT K CHANNELS. ((G.E. Kirsch[1,2], J.M. Pascual[1], and C.C. Shieh[1])) Departments of Molecular Physiology and Biophysics[1], and Anesthesiology[2], Baylor College of Medicine, Houston, TX 77030.

Mutation of the glycines in a conserved Gly-Tyr-Gly-Asp sequence in the P-region of voltage-gated K channels have identified determinants of ion selectivity. The function of the negatively charged Asp is not known because mutations at this position are not tolerated, owing to the four-fold replication of mutations in the tetrameric channel. We have successfully mutated $Asp^{378} \rightarrow Thr$ in a tandem dimer Kv2.1 construct to yield a two-fold neutralization of charge at this site. When expressed in *Xenopus* oocytes, the mutated channels showed markedly altered ion conduction and blockade, but nearly normal ion selectivity and macroscopic gating. Cation conduction in the inward direction was markedly curtailed, such that the instantaneous current-voltage relationship obtained in isotonic KCl, became strongly outwardly-rectifying. The sensitivity to block by external tetraethylammonium (TEA) was decreased more than 100-fold, without affecting sensitivity to internal TEA. Block by external Cs^+ was markedly reduced, as was the voltage dependence of the block. We conclude that Asp^{378} is part of a potassium ion binding site at the external mouth of the K pore. Supported by NIH grant NS29473.

Tu-AM-F6

PROBING THE PORE OF THE INWARDLY RECTIFYING K+ CHANNELS USING PERMEANT IONS. ((Reuveny, E. Jan, Y.N. and Jan, L.Y.)) Dept. of Physiology and HHMI, UCSF, San Francisco, CA 94143.

Inwardly rectifying (IR) potassium channels are very unique in their permeation properties. For example, they strongly interact with external and internal divalent cations in voltage- and flux-dependent manners and exhibit very strong ion selectivity for monovalent cations. A striking example of ion selectivity is the permeation of external Rb^+ ions through the pore, for example, voltage-gated K^+channels have much higher permeability to Rb^+ than IR channels. We were interested whether the properties of two different IR channel, IRK1 and ROMK1, which exhibit striking difference in their affinity to internal Mg^{2+} block, would have a difference in their permeability properties for Rb^+ ions. Replacing internal K^+ with Rb^+ ions shifted the reversal potential (E_{rev}) to more depolarized potentials. Using these values of E_{rev}, permeability ratios for Rb^+ relative to K^+ (P_{Rb}/P_K) were calculated for IRK1 and ROMK1 to be 0.39 and 0.64, respectively. We used this difference in P_{Rb}/P_K as a measuring tool to identify pore residues involved with the selectivity properties of IRK1 channel. Chimeric channel with the C-terminal and M2-transmembrane regions of ROMK1 into IRK1 were constructed, and measurement of P_{Rb}/P_K were performed. One channel construct showed a closer resemblance to ROMK1 than IRK1 in its selectivity to Rb^+, P_{Rb}/P_K=0.54. We currently in the process of narrowing down the specific residues involved in this action.

Tu-AM-F7

THE PORE OF *SHAKER* K CHANNELS CAN SIMULTANEOUSLY BE OCCUPIED BY AT LEAST THREE IONS. ((P. Stampe and T. Begenisich)) Dept. of Physiology, University of Rochester, Rochester, NY 14642. (Spon. by P. Stampe).

A test for independent ion movement through a pore may be made by determining the unidirectional ion influx (m_i) and efflux (m_o). For passive, independent ion movement, the ratio of these fluxes should be the ratio of the electrochemical activities of the ion on each side of the membrane: $\frac{m_o}{m_i} = \exp\left[\frac{(V_m - V_E)F}{RT}\right]$ If, however, ions interact in the permeation pathway, the right hand side of this equation is raised to a power, n'- the flux-ratio exponent. In the context of rate-theory models of permeation, this parameter may approach, but must be less than, the number of ions that may simultaneously occupy the pore. We measured unidirectional K^{42} fluxes through voltage-clamped *Xenopus* oocytes expressing ShBΔ6-46 channels. In each experiment one unidirectional flux was measured and the other obtained by subtraction from the ionic current. At -30 mV in 25 mM external K, both influx and efflux methods were used and n' values of 3.0 ± 0.16 (SEM, n=5) and 3.2 ± 0.52 (3) were obtained. Influx experiments yielded n' values of 2.5 ± 0.17 (9) and 2.1 ± 0.22 (3) at -15 and -5 mV, respectively (also with 25 mM external K). These values of the flux-ratio exponent indicate that the pore in *Shaker* K channels can simultaneously accommodate at least three ions.

Tu-AM-F8

EXTERNAL BARIUM BLOCK IS ALTERED BY AMINO ACID SUBSTITUTIONS AT THE OUTER PORE OF THE *SHAKER* POTASSIUM CHANNEL. ((R.S. Hurst, L. Toro, and E. Stefani)) Dept. of Anesthesiology, UCLA, 90024. (Spon. by L. Birnbaumer)

External barium inhibits potassium current in oocytes expressing the non-inactivating deletion of the *Shaker* potassium channel ShH4-IR (ShH4 Δ6-46). Block is comprised of a fast and slow component. The fast blocking component has a lower sensitivity (K_d > 20 mM, n = 3) and occurs quasi instantaneously. The apparent dissociation constant of the slow component has a dependence on holding potential which suggests that barium crosses approximately 25% of the electrical field to reach its binding site ($z\delta$ = 0.5). When holding at -90 mV the K_d of the slow component is 1.4 ± 0.2 mM (n = 4). An amino acid substitution at the outer mouth of the pore in ShH4-IR removing a hydroxyl group, Thr to Val at position 449 (T449V), decreased the affinity of the slow blocking component by approximately 4 fold (K_d = 4.1 ± 0.6, n = 4, HP -90). Introducing a bulkier, yet polar Tyr residue at this position (T449Y) completely eliminated the slow component of block (n = 3). Neither mutation had a significant effect on the fast blocking component. Previous studies have shown that the position equivalent to 449 in ShH4 is involved in the block by external tetraethylammonium (TEA) in potassium channels sensitive to this compound (Kavanaugh et al., 1991, *J. Biol. Chem.* 266:7583; MacKinnon and Yellen, 1990, *Science* 250:276). Block by external TEA is virtually independent of membrane potential in channels with a high affinity receptor. In contrast, external barium experiences an apparent electrical distance (δ) of 0.25 (slow component only). This suggests that barium binds deeper within the pore than TEA. Possibly, amino acid substitutions at position 449 in ShH4-IR influence the access of barium ions to a binding site deeper in the pore.
(supported by NIH grant GM50550 to ES and LT)

Tu-AM-F9

ALTERED MULTI-ION PROPERTIES ARISING FROM MUTATIONS IN THE PORE OF AN L-TYPE Ca^{2+} CHANNEL ((WA Sather, I Nussinovitch, DJ Gross, J Yang & RW Tsien)) Dept. Mol. & Cell. Physiol., Stanford Univ, Stanford, CA 94305

Each of the four internal repeats of voltage-gated Ca^{2+} channels contributes a single glutamate residue to a pore locus important for ion selectivity and permeation. We have studied effects of Asp, Gln and Ala substitution at these positions and find that some mutations have profound effects on multi-ion properties. Multi-ion interactions were assessed by measuring the voltage- and $[Ba^{2+}]$-dependence of single L-type Ca^{2+} channels exogenously expressed in Xenopus oocytes. Single channel *i*-V relations for wild-type (WT) channels are essentially linear over a range of $[Ba^{2+}]$ (10-110 mM) and membrane potential (-100 to 0 mV). Replacement of the repeat III Glu by Gln or Ala (but not Asp) gives rise to appreciable inward rectification, suggesting that these mutations can significantly alter the energy profile experienced by permeating divalent ions. Some mutations not only affect the pore's ability to bind a single divalent ion with high-affinity, as previously demonstrated, but also change its much weaker interactions with additional divalent ions. This was seen in two ways. First, the $[Ba^{2+}]$-dependence of single channel current was shifted to higher $[Ba^{2+}]$ with an Ala substitution in repeat II or a Gln substitution in repeat III (but not Asp or Ala substitution in repeat III), indicating a reduced binding affinity for multiple Ba^{2+} ions. Second, changes were also seen in the ability of Ba^{2+} to accelerate unbinding of pore-blocking ions. For example, enhancement by external Ba^{2+} of the rate of Cd^{2+} unblock required much higher $[Ba^{2+}]$ in the repeat II Ala mutant than in WT. This implies that the cluster of glutamates can support simultaneous interactions with more than one divalent cation, consistent with requirements for its mediation of efficient channel performance.

PROTEINS I

Tu-AM-G1

NEUTRON DIFFRACTOMETERS FOR STRUCTURAL BIOLOGY AT SPALLATION SOURCES: Benno P. Schoenborn, Los Alamos National Laboratory, Los Alamos, New Mexico 87545

Spallation neutron sources are ideal for diffraction studies of proteins and oriented molecular complexes. Experiments have shown that protein crystallography with a stationary crystal and a tailored wavelength band width reduces data collection time by increasing the diffraction signal -- the reciprocal lattice points are 'scanned' by the band width instead of rotating the crystal. This wavelength band width should be wide enough but not larger than the width needed to cover reciprocal lattice points; larger band width as used in the conventional Laue technique increases background significantly. With spallation neutrons and its time dependent wavelength structure it is easy to electronically select data with an optimal band width and cover the whole Laue spectrum as time (wavelength) resolved snap shots. This optimizes data quality with best peak to background ratios and provides adequate spatial and energy resolution to eliminate peak overlaps. The application of this concept to membrane and protein diffraction spectrometers will use choppers to select the desired Laue wavelength spectrum and employ focusing optics and large cylindrical Helium detectors to optimize data collection rates. These diffractometers will cover a Laue wavelength range from about 1 to 6 Anstoms with a flight length of 10 meters and an energy resolution corresponding to approximately .25A.

Tu-AM-G2

STRUCTURE AND STABILITY OF A SECOND MOLTEN GLOBULE APOMYOGLOBIN FOLDING INTERMEDIATE. ((S.N. Loh and R.L. Baldwin)) Department of Biochemistry, Stanford University, Stanford, CA 94305-5307.

Apomyoglobin folding is known to proceed through a molten globule intermediate (I_1) that is observed in both kinetic (pH 6) and equilibrium (pH 4) folding experiments. Of the eight helices in myoglobin, three (A, G, H) are structured in I_1 while the rest are unfolded. Here we characterize a second intermediate (I_2) which is induced either from the acid-unfolded protein (U) or from I_1 by ≥ 5 mM sodium trichloroacetate (see Goto et al., *Biochemistry 29*, 3480; 1990). Circular dichroism measurements monitoring urea- and acid-induced unfolding indicate that, compared to I_1, I_2 is more highly structured as well as more stable relative to U. Although I_2 exhibits properties closer to those of the native protein, 1D NMR spectra show that it maintains the lack of fixed tertiary structure that is the hallmark of a molten globule. Amide proton exchange coupled with heteronuclear 2D NMR are used to identify the source of the extra helicity observed in I_2. The results reveal that the existing A,G and H helices present in I_1 have become more stable in I_2, and that a fourth helix—the B helix—has been incorporated into the molten globule. The implications of this finding towards understanding the folding pathway of apomyoglobin are discussed.

Tu-AM-G3

STUDIES OF EARLY EVENTS IN THE FOLDING OF THE β-SHEET OF THIOREDOXIN BY FRAGMENT COMPLEMENTATION. ((María Luisa Tasayco, Timothy Anukele, Jian-Hua Li and Marie Christine Petit)) Department of Chemistry, City College of the City University of New York, New York, NY 10031. (Spon. by A. R. Srinivasan)

Structural studies of proteins at atomic resolution have shown that the extension of a β-sheet can mediate protein-protein or protein-peptide intermolecular interactions. Likewise, the folding of a β-sheet might start at a local region and subsequently extend to the rest of the polypeptide chain. The lack of ultrafast techniques with high structural resolution still precludes the direct observation of the early events in protein folding. The study of complementary protein fragments and their native-like complexes constitute an alternate indirect approach to gain insight about early folding intermediates or nucleation sites. To test the extension of a β-sheet within a protein as a folding mechanism, we chose to study the domain-sized complementary fragments (1–73, 74–108) of thioredoxin, a twisted β-pleated sheet flanked on either side by helices. The individual fragments and their native-like complex have been studied by molecular sieve chromatography, circular dichroism, fluorescence and multidimensional NMR spectroscopy. Our results suggest that the preorganized N-domain of thioredoxin provides a recognition surface for the folding of the C-domain with the subsequent formation of the antiparallel $\beta_2\beta_4$ strand between domains, and thus with extension of the β-sheet from the N- into the C-domain.

Tu-AM-G4

NMR ANALYSIS OF THE EQUILIBRIUM FOLDING PATHWAY OF STAPHYLOCOCCAL NUCLEASE. ((Y. Wang, J. Gillespie and D. Shortle)) Department of Biological Chemistry, The Johns Hopkins University School of Medicine, Baltimore, MD 21205

NMR methods are being used to follow the sequential build up of structure in the denatured state of staphylococcal nuclease as "the free energy distance" between the native and denatured states is varied by different perturbations of solution conditions (e.g., urea or glycerol concentration) or by changes in amino acid sequence. As one alternative to the conventional kinetic approach, an experimental and theoretical framework based entirely on time-averaged structures formed under equilibrium conditions provides a more realistic opportunity to quantitate the relative strengths and interdependencies of the many chain-chain interactions involved in protein folding. Extensive characterization of the large fragment $\Delta 131\Delta$, which serves as a model of a low-density denatured state, has revealed the presence of moderate amounts of native-like secondary structure. NMR structural analysis and distance mapping with covalently attached nitroxide spin labels are providing a picture of the interactions between these secondary structural elements. Results to date on the structure of $\Delta 131\Delta$ support a model in which native-like substructures form and combine in a pattern of hierarchical clustering steps.

Tu-AM-G5

Dimeric Form of Staphylococcal Nuclease from a 6 Amino Acid Deletion
Susan M. Green, Apostolos G. Gittis, Alan K. Meeker and Eaton E. Lattman. Dept. of Biophysics and Biophysical Chemistry, The Johns Hopkins University School of Medicine, 725 N. Wolfe Street, Baltimore, MD 21205

A mutant form of staphylococcal nuclease, resulting from the spontaneous deletion of residues 114-119, has been characterized. Residues 114-119 make up the loop leading to the C-terminal helix in wild-type nuclease. The mutant shows a loss in stability of 2.6 kcal/mol relative to wild-type nuclease (5.5 kcal/mol). CD demonstrates slight changes in secondary structure. Interestingly, the kinetics of refolding show time constants of 109 and 460 seconds, much greater than the milliseconds required for refolding of wild type. Equilibrium ultracentrifugation demonstrates that this mutant forms a stable dimer, with $K_D \sim 1 \times 10^{-8}$ M. To determine the nature of the dimeric interface, the X-ray crystal structure was solved. The protein crystallizes in space group $P4_12_12$ with lattice constants of a= b= 132.3 Å, c=54.8 Å and two monomers per asymmetric unit. Data were collected on an R-Axis IIC at -160 °C to a resolution of 1.85Å. The crystal structure was determined by molecular replacement using AMORE (J. Navaza) and subsequently refined using XPLOR (A. Brünger). The current model has a crystallographic R-factor of 16.9 % to a resolution of 2.0 Å. and contains 138 water molecules. In the dimer structure, the C-terminal helix is stripped from its own monomer, swapping places with the helix on the adjoining monomer. That such a tightly associating dimer can result from a spontaneous mutation has important implications for the evolution of oligomers.

Acknowledgments: We thank David Shortle. Supported by NIH grant GM-36558 and The Lucille P. Markey Charitable Trust.

Tu-AM-G6

KINETIC ACTIVATION MORE THAN THE STABILITY OF FOLDING INTERMEDIATES DETERMINES PATHWAYS OF PROTEIN FOLDING.
((T.Y. Tsong, Z.-D. Su and H.-M. Chen)) Dept of Biochem, Hong Kong Univ of Science & Technology, Clear Water Bay, Kowloon, Hong Kong.

If folding of a peptide chain is driven by the stability of folding intermediates, it will proceed in parallel with the free energy gain of these intermediates. If folding is dictated by kinetic barriers, it will be guided through the valley of the least activation energies irrespective of the stability of folding intermediates. Our previous study of folding of the acid- and base-denatured staphylococcal nuclease (SNase) indicates that folding proceeds via a sequence of intermediates which exhibit similar free energies. This result upholds the kinetic activation model. However, the acid- and the base-denatured SNase retain considerable sheet-like chain conformations, and effects of these residual structures on folding mechanisms could not be assessed. Here we show that folding of the GuHCl-unfolded SNase (with no residual structures) also follows similar kinetics. Kinetics in the time range 20 ms (mixing time of the CD attachment of Applied Photophysics stopped-flow) to 500 s were monitored with CD from 220 nm to 240 nm, which measures the extent of secondary structure formation. At 25°, for the time resolved signals, the unfolding at 2.0 M GuHCl was monophasic (1.7 s) and the folding at 0.34 M GuHCl was triphasic (430 ms, 6.2 s, and 32 s). These results agree with the previously proposed kinetic scheme, $D_3 \Longleftrightarrow D_2 \Longleftrightarrow D_1 \Longleftrightarrow N_0$, in which the 3 Ds are the 3 sub-states of the unfolded state and N_0 is the native state. The ΔG for the $D_3 \Longleftrightarrow D_2$ was slightly positive (< 0.1 kcal/mol), for the $D_2 \Longleftrightarrow D_1$ was -0.5 kcal/mol, and for the $D_1 \Longleftrightarrow N_0$ was -6 kcal/mol. Although the 3 Ds are iso-energetic, the folding pathway was unique - there was no stochastic conversion among the 3 sub-states. These data lend further support to the kinetic activation model. We have determined the CD spectrum of each intermediate with the stopped-flow method. Spectral changes too fast or too slow to resolve were also measured. Ref: Biochem. 31:1483 (1992); 31:12369 (1992); BJ. 66:40 (1994).

Tu-AM-G7

PHOSPHORESCENCE REVEALS A CONTINUED SLOW ANNEALING OF THE HYDROPHOBIC CORE OF *E. COLI* ALKALINE PHOSPHATASE FOLLOWING REACTIVATION.
((V. Subramaniam†, N. C. H. Bergenhem‡, Ari Gafni‡ and D. G. Steel§)) Institute of Gerontology, †Applied Physics Program, ‡Department of Biological Chemistry, §Departments of Physics and Electrical Engineering, University of Michigan, Ann Arbor, MI 48109.

When *Escherichia coli* alkaline phosphatase (AP) is refolded *in vitro* after extensive denaturation in 6.2 M guanidine hydrochloride (GuHCl), the enzymatic activity reaches its asymptotic value in one hour at 24°C. In contrast, the structural rigidity of the hydrophobic core of the protein, measured by the recovery of tryptophan phosphorescence lifetime, returns to its characteristic native-like value over several days. Moreover, the global protein stability, measured by the rate of inactivation in 4.5M GuHCl, also increases on a time scale much longer than the recovery of activity. In the context of the rugged energy landscape model of Frauenfelder et al.(1), the slow annealing of the hydrophobic core is consistent with the presence of high energy barriers that separate fully active intermediates along the folding pathway. These results clearly demonstrate that although the return of enzymatic activity, the traditional measure of the attainment of the native state, indicates that AP has refolded to its final, active, conformation, the phosphorescence data indicate otherwise. The data suggest that the core of the protein undergoes continued structural rearrangements increasing the rigidity of the protein environment surrounding the emitting tryptophan long after the return of enzyme activity. [NIA AG09761; ONR N00014-91-J-1928]

1. H. Frauenfelder, S. G. Sligar, P. G. Wolynes, *Science* **254**, 1598-1603 (1991).

Tu-AM-G8

LONG RANGE LOOPS REDUCE THE ENTROPY IN THE EARLY FOLDING INTERMEDIATES OF BPTI.
((V. Itah and E. Haas)) Dept. of Life Sciences, Bar-Ilan University, Ramat Gan 52900, Israel.

A search for the early folding intermediates in unfolded and partially folded states of reduced bovine pancreatic trypsin inhibitor (BPTI) was done by means of dynamic time resolved non-radiative excitation energy transfer (ET) measurements. The experiments were designed to determine the topology of the backbone and the local folding transitions in the partially folded states. Four double labeled BPTI derivatives were used in which the donor was attached to the N-terminal arginine residue and the acceptor was specifically attached to one of the lysine residues. The pairs of sites, residues 1 and 26 and residues 1 and 46 showed close proximity in the dominant sub-population in the unfolded states. These contacts form loops of 26 and 46 residues.

These results show that a very effective early step in the folding of BPTI is the stabilization of long range loops by non-local interactions (NLIs) between the terminal chain segments and between the N-terminal segment and the ß structure in the center of the polypeptide backbone.

These observations are interpreted as an indication that in the case of BPTI, stabilization of long range loops by specific NLIs facilitate the accelerated folding into a native topology, within the early steps of the folding pathway. Very early loop formation by specific NLIs can be a key factor in solving the Levinthal paradox and in determining the steps which direct the folding pathway. The loops are generated by loose cross-links between pairs of specific sites (pairs of single residues or short stretches of the chain). Formation of loops is a very effective mean of reducing chain entropy at the expense of a minimal number of very stable interactions.

Tu-AM-G9

UNFOLDING OF RNase A ON THE PICOSECOND TIMESCALE IN RESPONSE TO A LASER-INDUCED TEMPERATURE JUMP
((C. M. Phillips, Y. Mizutani and R. M. Hochstrasser)) Department of Chemistry and Regional Laser and Biotechnology Laboratories, University of Pennsylvania, Philadelphia, PA 19104-6323.

Using a new ultrafast temperature jump method for aqueous protein solutions, we are investigating the earliest structural changes associated with the unfolding of bovine pancreatic Ribonuclease A (RNase A). A Nd:YAG laser based temperature jump apparatus pumps an absorbing dye in aqueous solution and creates a bulk solution T-rise in water on the 10's of picoseconds timescale. This temperature rise induces a structural unfolding in RNase A. These changes are monitored with a time resolution ca. 50 ps, by infrared radiation in the Amide I region (1600-1700 cm^{-1}). Precise thermometry can be performed simultaneously on the pumped region since there are known temperature dependent changes in the infrared spectrum of D_2O which produce a measureable background. Distinct spectral changes have been seen for the protein which begin ca. 1000-1200 ps after the T-jump. By tuning the infrared radiation we obtained a spectrum of the protein. At 3.5 ns into unfolding the time-resolved spectrum differs from the equilibrium difference spectrum in the β-sheet region whereas the α-helix and bends regions are similar. The kinetic results indicate that the β-sheet structure signal at 1630 cm^{-1} is diminished more slowly than the growth of the 1666 cm^{-1} signal, corresponding to α-helix, bends and turns.

Supported by NIH grant RR 01348.

Tu-AM-G10 *(See Th-PM-C3)*

Tu-AM-H1

ENERGY FLUXES AND PROPAGATION OF DISTORTION PRODUCTS IN THE COCHLEA. ((V. S. Markin and A. J. Hudspeth)) Howard Hughes Medial Institute and Center for Basic Neuroscience Research, University of Texas Southwestern Medical Center, Dallas, TX 75235-9117.

The propagation of acoustic signals in the cochlea has been mathematically described in terms of energy fluxes (J. Lighthill, in *Mechanics of Hearing*, 1981). The equation of energy includes the terms describing losses due to viscous drag and inputs due to active processes in the cochlea or exchange of energy between different signals. For a single traveling wave, this approach reproduces the well known build-up of oscillation amplitude in the basilar membrane near the local resonant frequency and a sharp drop in the signal's amplitude thereafter. The interaction of traveling waves of different frequency ($f_1<f_2$) gives rise to the distortion products. The cubic distortion product $2f_1-f_2$ is generated in the region of the cochlea between characteristic frequencies f_2 and f_1 and then propagates to its own characteristic place. During this propagation, the amplitude of the distortion product is strongly amplified. We analyzed possible mechanisms of primary-tone interaction and found the dependence of distortion products on the difference between the primary-tone frequencies and on their amplitudes.

This research was supported by National Institutes of Health grant DC00317.

Tu-AM-H2

Light illumination enhances the efficiency of signal transduction to hydrodynamic stimulation in the caudal photoreceptor cells of crayfish sixth ganglia. ((Xing Pei, Lon Wilkens and Frank Moss)) Dept. Physics and Biology, University of Missouri at St. Louis. St. Louis, Mo 63121.

The caudal photoreceptor (CPR) cells found in the sixth ganglion of crayfishes are complex multi-modal interneurons. The CPR cells respond to light with tonic spike discharges. They receive and process input from an array of tactile hair cells (mechanic receptors) located on the tail fan and have direct access to locomotory centers. Multi-sensory information is integrated and processed by these cells. We have performed experiments using weak hydrodynamic stimuli across the array of mechanoreceptors while recording the spike discharges from the CPR cells exposed to several different light intensities. Interval histograms were constructed from spike trains. Signal-to-noise ratios and mean discharge rates were extracted from recordings. We observed a remarkable, non-linear, increase in signal-to-noise ratios with increasing light intensity, especially for weak stimuli. From a dark environment to under light illumination, the mechano-sensitivity of CPR cells was improved with a lowing of threshold ~ 5 dB and an increase of response to mechanical stimuli. The histogram of discharge intervals also changed from gamma like to gauss like distribution. These results are further discussed with simulated data from a threshold analog electronic model and may be interpreted by the mechanism of stochastic resonance.

Tu-AM-H3

EXPERIMENTAL EVIDENCE THAT MECHANOSENSITIVITY OF THE BACTERIAL LARGE-CONDUCTANCE MS CHANNEL (MscL) IS DETERMINED BY HYDROPHOBIC INTERACTIONS WITHIN THE CHANNEL COMPLEX. ((S.I. Sukharev, P. Blount, S. Nagle and C. Kung)) Laboratory of Molecular Biology, University of Wisconsin, Madison, WI 53706

A gene encoding a 2.5 nS mechanosensitive channel of large conductance (MscL) from *E. coli* has recently been cloned (*Nature*, **368**, (1994) 265). The functional channel has been proposed to be a homomultimer of several 15 kD subunits. Each subunit consists of two putative hydrophobic membrane-spanning domains and a hydrophilic C-terminus. Here we present evidence that hydrophobic interactions are involved in the gating of the MscL channel. First, expression of MscL with 25 C-terminal residues deleted revealed a functional MS channel, suggesting that the first 3/4 of the protein, predominantly hydrophobic, is sufficient for channel activity. Second, single-channel recording of highly purified MscL reconstituted into liposomes revealed that open probability (P_o) can be substantially influenced by agents affecting hydrophobic interactions. Perfusion of patches kept at a constant hydrostatic pressure (**p**) with salting-out (stabilizing) agents inhibited MscL activity, whereas chaotropic agents that weaken hydrophobic interactions, dramatically activated the channel. Both effects were reversible and resulted in corresponding positive or negative shifts of P_o(**p**)-curve along the **p** axis. The data suggest that channel opening is a result of stretch-induced breakage of hydrophobic interactions between certain protein domains. The energy gain from the exposure of these domains to water should close the channel when the mechanical stimulus is off. Accounting the role of hydrophobic interactions in channel's mechanical compliance may bring some corrections to Hookean models of MS channel gating. Supported by NIH GM47865.

Tu-AM-H4

EFFECTS OF A WEAK ACID ON GATING OF MECHANOTRANSDUCING ION CHANNELS IN C6 GLIOMA CELLS. ((C.L. Bowman[1] and J. W. Lohr[2])). 1. Department of Biophyscial Sciences, SUNY-Buffalo, NY. 2. VAMC, Buffalo, NY. 14214.

It is commonly found that mechanotransducing (MS) ion channels quickly activate following a rapid change in pipette pressure. In these cases where the pressure change and channel activation is tightly coupled, MS channel activity adapts (Hamill and McBride, Jr., 1992; Bowman and Lohr, 1993). On the other hand, recent work from C. E. Morris' laboratory shows that substantial delays in channel activation exist. Using C6 glioma cells, we demonstrate that quick and slow activation can be observed in the same cell-attached patch, and that Na acetate modulates both adaptation and activation. In cell-attached patches, the onset of channel activity and subsequent adaptation usually remains constant for periods of 30 minutes with continuous perfusion of 100 mM NaCl Ringer's solution. Switching to 10 mM, 33 mM or 100 mM Na acetate (with corresponding decreases in [NaCl]) reduces adaptation of MS channels, and causes substantial increases in delay in onset of channel activity in cell-attached patches. Residual MS channel activity following adaptation is enhanced. Washout of Na acetate enhances the effects observed in the presence of Na acetate. These results suggest that acidosis and/or events related to swelling regulates the gating of MS channels by possibly altering cytoskeletal elements. A mechanical model will be presented.

Tu-AM-H5

EVIDENCE FOR VOLTAGE-SENSITIVE CA^{2+}-CONDUCTING CHANNELS IN AIRWAY EPITHELIA. ((Michael Woodruff, Scott Boitano and Ellen Dirksen)) Dept. of Anat. and Cell Biol., UCLA School of Medicine, LA CA 90024.

Using fura-2 imaging-microscopy of intracellular Ca^{2+}, $[Ca^{2+}]_i$, we have obtained evidence that mechanical stimulation of a single cell in airway epithelial cultures initiates a flux of Ca^{2+} across the plasma membrane through the opening of Ca^{2+}-conducting channels. The flux is blocked by several voltage-sensitive Ca^{2+}-channel blockers, including Ni^{2+} and the dihydropyridines nifedipine and nimodine. Addition of BayK-8644 (2 μM) leads to an increase of $[Ca^{2+}]_i$. Addition of high extracellular K^+ (55 mM), to depolarize the plasma membrane, causes an increase in $[Ca^{2+}]_i$ that is inhibited by 1 mM Ni^{2+}. Membrane voltage changes can be monitored during mechanical stimulation by intracellular recording. Mechanical stimulation leads to a rapid depolarization of the stimulated cell. These mechanically-induced voltage changes can be attenuated by adding K^+-ionophore valinomycin. Similarly, when $[Ca^{2+}]_i$ is monitored by digital image-microscopy in Ca^{2+}-free solutions, in the presence of valinomycin, mechanically-induced Ca^{2+} efflux from the stimulated cell is blocked. These results suggest voltage-sensitive Ca^{2+}-conducting channels exist in the plasma membrane of airway epithelial cells and these channels contribute to $[Ca^{2+}]_i$ changes following mechanical stimulation of a single cell. *S.B. is a Parker B. Francis Family Fellow. This research was supported by the Smokeless Tobacco Research Council, Inc. and the Tobacco Related Disease Research Program of the University of California*

Tu-AM-I1

PARTIAL BLOCK OF RAT MUSCLE SODIUM CHANNELS BY AN ANALOG OF μ-CONOTOXIN. ((R.J. French and R. Horn)) Dept of Medical Physiology, Univ of Calgary, Calgary, Alberta, Canada, T2N 4N1; Dept of Physiology, Jefferson Med College, Philadelphia, PA 19107.

μ-Conotoxin (μCTX) is a 22 amino acid peptide that causes all-or-none block of Na channels of adult skeletal muscle. In the analog, R13Q, glutamine replaces arginine-13 of μCTX. R13Q, unlike other analogs, produces a partial block of rat muscle Na channels in bilayers (Becker et al., *Biochem* 31:8229, 1992). When bound, R13Q reduces the single channel current amplitude to 25-30% of the unblocked level. Because of possible channel modifications of the batrachotoxin used in bilayer experiments, we examined the block by R13 analogs of cloned Na channels of rat skeletal muscle (rSkM1), expressed transiently in a mammalian cell line and studied with whole cell recording. Dose-response curves, using concentrations up to 200 μM, show that R13Q blocks Na current with an IC_{50} of 7.4 μM, by comparison with ~50 nM for native μCTX. However, saturating doses of R13Q reduce the current to ~25% of its peak value at 0 mV, consistent with bilayer experiments; this residual current is similar in kinetics and voltage dependence to the current in absence of blocker, except that the peak current-voltage relationship is shifted ~10 mV in the depolarizing direction. Charge-conserving substitutions for R13 (lysine: IC_{50}=575 nM; ornithine: IC_{50}=286 nM) reduce the potency of μCTX, but these analogs appear to produce a complete block of rSkM1 Na current at saturating concentrations. Glutamate substitution for the adjacent aspartate (D12E) reduces μCTX potency (IC_{50}=5.5 μM; Chahine et al, *Biophys J* 66:A103, 1994), partially due to its interaction with R13 (*ibid*), but can block completely. Thus a cationic residue at position 13 appears to be necessary for complete block.

Tu-AM-I2

COUPLING OF VOLTAGE AND INACTIVATION IN NA CHANNELS. ((M.E.O'Leary, L.-Q. Chen, R.G. Kallen and R. Horn)) Dept of Physiol, Jefferson Medical College, Philadelphia, PA 19107; Dept of Biochem. & Biophysiol., Univ. of Penn., Philadelphia, PA 19104.

The inactivation of the Na channels that generate action potentials is voltage dependent. We show that a pair of tyrosine residues, on the cytoplasmic linker between the 3rd and 4th domains of human heart Na channels, is linked to voltage sensors that respond to depolarization. Substitution of these residues by glutamine (YY/QQ), but not phenylalanine, eliminates the voltage dependence of the inactivation time constant for voltages more positive than -60 mV. This double mutation increases the rate of recovery from inactivation and decreases the voltage dependence of all steady-state and kinetic properties of inactivation. Single channel measurements show that the latencies for a channel to open after a depolarization are faster and less voltage dependent in YY/QQ than in wild-type channels. The YY/QQ mutations also decrease the lag in development of macroscopic inactivation after a depolarization. The data suggest that in wild-type channels depolarization has two consequences for inactivation. The first is a rapid increase in the affinity of a docking site for the cytoplasmic inactivation gate, as observed in potassium channels. The second consequence, apparently novel to Na channels, is the slower movement of the inactivation gate *via* attachment of these tyrosines to a voltage sensor. Inactivation is slowed at negative voltages and accelerated at more positive voltages by this coupling mechanism.

Tu-AM-I3

EVIDENCE FOR FUNCTIONAL ASSOCIATION OF THE β_1 SUBUNIT WITH HUMAN HEART (hH1) AND RAT SKELETAL MUSCLE (μ1) SODIUM CHANNEL α SUBUNITS EXPRESSED IN *XENOPUS* OOCYTES ((H. Bradley Nuss, Gordon F. Tomaselli, and Eduardo Marban)) Dept. of Medicine, Johns Hopkins University, Baltimore, MD

Immunoaffinity studies have determined that native cardiac and skeletal muscle Na channels are complexes of α and β_1 subunits. While structural correlates for activation, inactivation, and permeation have been identified in the α subunit and the expression of α alone encodes functional channels, β_1-deficient rat skeletal muscle (μ1) and brain Na channels do not gate normally. The requirement of a β_1 subunit for normal function of the human heart Na channel clone (hH1) has not yet been established. Coinjection of rat brain β_1 subunit cRNA with hH1 (or μ1) α subunit cRNA into *Xenopus* oocytes increased peak Na currents by 350% (250%) without altering the voltage dependence of activation. Coexpression of β_1 subunit shifts the voltage dependence of inactivation in oocytes to more negative potentials closer to the relationships found in native channels. Coinjection of β_1 subunit shifted the half-inactivation voltage to -80±1mV from -77±1 mV for hH1 Na channels (n=6,11, P<0.02) and induced a 6mV hyperpolarizing shift in μ1 Na channels (n=8,15, P<0.01). While hH1 Na channels have intrinsically faster inactivation kinetics than μ1 Na channels, coexpression with β_1 subunit speeded the decay of macroscopic current when quantified by time to 50% and 90% decay of peak current. Ensemble average currents from cell-attached patches confirmed that hH1 Na channels coexpressed with β_1 subunits have increased rates of inactivation. Use-dependent decay of peak hH1 Na current during repeated pulsing to -20mV (1s, 0.5Hz) following a long rest (>45s) was reduced to 16±2% of the first pulse current in oocytes coexpressing α and β_1 subunits (n=11) compared to 35±8% use-dependent decay for oocytes expressing the α subunit alone (n=10). Recovery from inactivation of hH1 Na currents after 10 ms and 1s pulses to -20mV occurred with two rate constants: coexpression of β_1 subunit decreased both fast and slow recovery rate constants. These data support an important functional association between the β_1 subunit and hH1 and μ1 Na channel α subunits.

Tu-AM-I4

STRUCTURAL DETERMINANTS OF NA^+ CHANNEL MODULATION BY β_1 SUBUNIT. ((N. Makita, P. B. Bennett and A. L. George)) Departments of Medicine and Pharmacology, Vanderbilt University School of Medicine, Nashville, TN 37232

A recombinant human skeletal muscle Na^+ channel α subunit (hSkM1) exhibits slow inactivation when expressed in *Xenopus* oocytes, while the human heart α subunit (hH1) inactivates rapidly. Co-expression of β_1 subunit restores normal rapid inactivation in hSkM1, but has no detectable effect on hH1. To identify specific regions of the α subunit responsible for this modulation, we constructed chimeric channels by interchanging regions of these two channel isoforms. Chimera SH consists of N-terminus (NT) through interdomain 23 (ID23) of hSkM1 and domain 3 (D3) through C-terminus (CT) of hH1, while chimera HS has NT through ID23 of hH1 and D3 through CT of hSkM1. Channels were expressed in *Xenopus* oocytes in the presence or absence of human β_1 subunit (β_1), and assayed by 2-electrode voltage clamp recording. Steady-state inactivation curves were fitted with the Boltzmann equation. The $V_{1/2}$ of the chimeras were similar but intermediate between wild type (WT) hSkM1 and hH1 ($V_{1/2}$ (mV); hSkM1:-51±0.7, hH1:-79±0.4, SH:-65±1, HS:-67±1). β_1 did not change the $V_{1/2}$ of either chimera. Unlike WT-hSkM1, the fraction of SH channels recovering slowly from inactivation was not affected by the β_1 subunit (-β_1: 0.33±0.05 vs. +β_1: 0.29±0.03; N=9). The fraction of slowly recovering channels was smaller in HS (0.14±0.02) than SH. The β_1 subunit further significantly reduced this slow component (0.07±0.01, N=7, p<0.01), leading to an acceleration of recovery from inactivation. The effect of β_1 subunit on the onset of inactivation was also markedly different in the two chimeras. SH was unaffected by β_1 whereas inactivation of HS was accelerated (Fig). These results suggest that the principal region of hSkM1 required for interaction with β_1 subunit is localized to the carboxyl terminal half of the α subunit molecule.

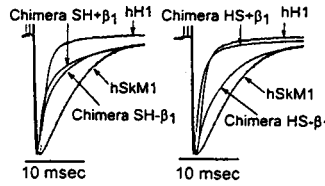

Tu-AM-I5

SODIUM CHANNEL INACTIVATION FROM CLOSED STATES; EVIDENCE FOR AN INTRINSIC VOLTAGE DEPENDENCE OF THE CLOSED TO INACTIVATED TRANSITION RATE CONSTANTS. ((L. Goldman)) Dept. of Physiology, School of Medicine, Univ. of Maryland, Baltimore, MD 21201.

The time course of sodium channel inactivation from closed states in inside-out excised patches from neuroblastoma N1E 115 is well described by a single exponential. Mean time constants at 7.5 ± 0.5°C were 15.14 ms at -50, 20.12 ms at -60, 29.56 ms at -70, and 66.42ms at -80mV. Mean steady state values were 0, 0.035, 0.098 and 0.321. Means of zero time intercepts were never far from unity at any potential. Overall mean was 0.993. A two closed, one conducting, and one inactivated state scheme predicts a zero time intercept greater than unity if only the closed state closest to conducting directly inactivates, and less than unity if only that furthest from conducting does, while experiments indicate a zero time intercept at or near unity. Relative amplitude of the predicted exponential components is determined in whole or part by relative size of the two time constants. One possibility is that any additional component is too fast to resolve. A second is that both closed states directly inactivate. If closed to inactivated rate constants are similar for both closed states, the amplitude of any additional component is arbitrarily small. If they are identical, closed state inactivation develops as a single exponential with a unity zero time intercept. Time constants were fitted to the initial delay in activation development of ensemble average currents (four patches at -50, one at -60mV) to estimate the time constant of exchange between closed states. Mean at -50 was 1.98ms (13.1% of closed state τ), and 1.97ms at -60 (9.8% of closed τ), readily discriminable differences suggesting transitions to the inactivated state proceed from all closed states with very similar or identical rate constants. Means of closed to inactivated rate constants were 0.0108 ms^{-1} at -80 and 0.0690 ms^{-1} at -50mV, an inherent voltage dependence with this interpretation.

Tu-AM-I6

CLONING OF A NOVEL SODIUM CHANNEL ALPHA-SUBUNIT FROM SCHWANN CELLS. ((S.M. Belcher, C. Zerillo, J.M. Ritchie, R. Levenson*, and J.R. Howe)) Department of Pharmacology, Yale Univ. School of Medicine, New Haven, CT 06520 *Department of Pharmacology, The Milton S. Hershey Medical Center, Penn State College of Medicine, Hershey, PA 17033.

Whereas voltage-gated sodium channels are responsible for the mediation of neuronal excitability, the expression of these channels is not restricted to excitable cells. Several years ago, Ritchie and his colleagues showed that Schwann cells express Hodgkin-Huxley-type sodium channels that have similar, but not identical, properties to those found in excitable cells (*TINS* 15, 345-350, 1992). These results suggested the possibility that Schwann cells express a novel sodium channel isoform.

Using a combination of cDNA cloning from a rabbit Schwann cell library and RT-PCR based approaches, we have cloned and sequenced nearly the entire coding sequence of a novel sodium channel α-subunit. Comparison of the predicted amino acid sequence of the Schwann cell isoform with the sequence of other sodium channel α-subunits reveals that the Schwann cell isoform is most similar to the brain type II isoform (~85% amino acid identity) and is most dissimilar to the glial specific isoform (NaG; ~50% identity). In order to rule out the possibility that we isolated the rabbit version of brain II, rather than a novel Schwann cell isoform, we have isolated a partial sodium channel cDNA clone corresponding to the rabbit brain type II α-subunit. This clone was isolated from a rabbit brain cDNA library and exhibits >97% amino acid identity compared with the rat brain type II sequence. In contrast, the rabbit brain type II clone is ~87% identical to the corresponding Schwann cell amino acid sequence. Experiments are in progress to determine whether expression of this novel isoform is restricted to Schwann cells.

Tu-AM-I7

IMMUNOLOCALIZATION OF THE mNa$_v$2.3 Na^+ CHANNEL IN HEART AND UTERUS. ((T.J. Knittle, K.L. Doyle, and M.M. Tamkun)) Dept. of Molecular Physiology and Biophysics, Vanderbilt Medical School, Nashville, TN 37232.

mNav2.3 is a putative voltage-gated Na^+ channel (NaCh) expressed in heart and uterus that shares only 45% amino acid sequence identity with NaChs from gene subfamily 1. Northern analysis revealed that mNav2.3 is the only cloned NaCh expressed in mouse uterus and the levels of mRNA significantly increased during the latter stage of gestation. To examine the cell-specific expression of mNav2.3 protein in mouse heart and uterus during gestation, rabbit polyclonal antibodies were raised against bacterially produced fusion proteins containing unique mNav2.3 sequence from the carboxyl terminus and the cytoplasmic linker connecting domains 2 and 3. Immunohistochemical (IHC) studies revealed that mNav2.3 expression in heart and quiescent uterus colocalized with only glial and nerve-specific antibodies. During late pregnancy, mNav2.3 expression in nerve disappeared concomitant with increased expression in both longitudinal and circular smooth muscle. Expression in uterine myocytes reached a maximum at term and quickly declined after delivery. In all experiments, identical IHC patterns were observed with antisera raised against both epitopes. IHC results are supported by Western analysis in which the 217 kDa NaCh increased during late pregnancy. These data are consistent with reported increases in uterine myocyte NaCh density during pregnancy. It is likely that mNav2.3 is the uterine NaCh first reported by Sperelakis et al. The function of mNav2.3 expression in the uterus during gestation and delivery remains to be determined.

Tu-AM-I8

DIFFERENTIAL EFFECT OF HALOTHANE ON Na^+ AND Ca^{2+} CHANNELS EXPRESSED IN *XENOPUS* OOCYTES. ((A. M. Correa and N. Qin)) Dept. of Anesthesiology, UCLA, Los Angeles, CA, 90024.

General anesthetics (GA) modify cell excitability in nerves and muscles by differential effects on ligand-gated and/or voltage-gated ion channels. The basic mechanisms involved are still unclear. The purpose of this work was to examine in detail the properties of V-dependent ion channels exposed to volatile anesthetics. The cut open oocyte technique was used to look at the effects of Halothane (**Hal**) on the kinetics and conductance properties of Na^+ and Ca^{2+} channels. *Xenopus* oocytes were injected with cRNA's encoding for the alpha (α) subunits of the skeletal muscle Na^+ channel (μI) and of the cardiac (α1C, N60 an N-terminal truncation) Ca^{2+} channels. Currents were recorded from oocytes expressing α subunits alone and α plus beta (β) subunits (β_1 for μI Na^+ and β_{1b} or β_{2a} for Ca^{2+} channels). Perfusates were pre-equilibrated (15-20 min) with **Hal** vaporized at 3% in O_2. I_{Na} currents were recorded in external 120 NaMES and internal 90 Cs_2SO_4. I_{Ca} currents were recorded in external 10 BaMES, 96 NaMES and internal 120 KMES. **Hal** did not affect the magnitude of Na^+ currents. There was no change in the slope conductance (G = 20 mS for α and 78 mS for $\alpha+\beta$) nor in the V-dependence of the peak I or of the fractional conductance. Only minor changes in kinetics were observed: activation and inactivation were faster than control. Conversely, Ca^{2+} currents were blocked $\simeq$50% with no apparent shift in the V-dependence of the current or of the fractional conductance. Results are consistent with L-type Ca^{2+} channel block by **Hal**. **Hal** also shifted the relative contribution of fast and slow components of α1C currents. The effects on I_{Na} and I_{Ca} currents did not depend on β subunits coexpression. These results support specific interactions of channel proteins with GA. NQ supported by NIH AR43411.

Tu-AM-I9

BIOFERROELECTRICITY IN THE SODIUM CHANNEL: CONFORMATIONAL CHANGE IN THE PROBABLE ACTIVE SITE. ((Vladimir S. Bystrov and H. Richard Leuchtag)) Institute of Mathematical Problems of Biology, Russian Academy of Sciences, Pushchino, 142292, Russia, and Department of Biology, Texas Southern University, Houston, TX 77004. (Spon. by M. Hillar)

The closed Na channel is in a nonequilibrium state due to the strong field of the resting potential. Depolarization leads to a transition to an ion-conducting open state. Interpretation of the transition as ferroelectric-paraelectric explains a number of electrical and thermal phenomena. The hypothesis is completed by the assumption that the open channel is a superionic conductor. The inward movement of this phase transition has been studied by a thermodynamic ferroactive model. The equation of motion yields a kink solution for the transition front. The primary structure of the Na channel suggests that the four S4 segments of the channel, acting as a unit, form the active site involved in voltage sensing and ion conduction. Electrostatic analysis shows that an S4 segment is unstable as an α helix without external forces, suggesting that the resting potential induces these forces. On depolarization the S4s are postulated to extend and become coordinated by mobile ions traversing them.

Tu-AM-I10

BIOFERROELECTRICITY IN THE SODIUM CHANNEL: MOLECULAR TILT AND CHIRALITY. ((H. Richard Leuchtag)) Department of Biology, Texas Southern University, Houston, TX 77004.

Ion channels are molecular components of membranes, which have the two-dimensional order of lyotropic smectic liquid crystals. The hypothesis of a ferroelectric unit in a sodium channel, which provides physical explanations for the open-closed transitions, gating currents and thermal phenomena, thus suggests a comparison with ferroelectric liquid crystals. These are known to be of the smectic C* type: elongated chiral molecules that are tilted at an angle to the layer normal. Since the probable active site and ferroelectric unit is the four-S4 bundle, the question becomes whether the S4s are tilted and the bundle chiral. Potassium-channel and other studies suggest a tilt of the S4 segments, and the conserved proline residues present in three of the Na-channel S4s bend the α helices, providing the necessary chirality. Thus the closed channel appears to satisfy the necessary conditions to be a component of a smectic C* ferroelectric liquid crystal. An electric-field-induced transition may then unwind the α helices, breaking their H bonds, to establish a new paraelectric structure coordinated by the permeant ions, the open channel.

EMULATION AND SIMULATION OF NEURONAL FUNCTION

Tu-PM-Sym-1

MODELLING AND MEASURING CA^{2+} DYNAMICS IN NEURONAL SIGNALLING. ((D.W. Tank)) AT&T Bell Labs., Murray Hill, NJ

Tu-PM-Sym-2

USE OF THE DYNAMIC CLAMP TO MODULATE NEURONS AND NETWORKS. ((E. Marder)) Brandeis Univ.